Urocortin-3 Neurons in the Mouse Perifornical Area Promote Infant-directed Neglect and Aggression

Anita E Autry[1,2], Zheng Wu[1,3], Vikrant Kapoor[1], Johannes Kohl[1,4], Dhananjay Bambah-Mukku[1], Nimrod D Rubinstein[1,5], Brenda Marin-Rodriguez[1], Ilaria Carta[2], Victoria Sedwick[2], Ming Tang[1,6], & Catherine Dulac[1]

[1] Howard Hughes Medical Institute, Department of Molecular and Cellular Biology, Center for Brain Science, Harvard University, Cambridge, Massachusetts 02138, USA.

[2] Dominick P. Purpura Department of Neuroscience, Department of Psychiatry and Behavioral Sciences, Albert Einstein College of Medicine, Bronx, NY 10461, USA.

[3] Current Address: Mortimer B. Zuckerman Mind Brain Behavior Institute and Department of Neuroscience, Columbia University, New York, NY 10027, USA.

[4] Current Address: The Francis Crick Institute, London, UK.

[5] Current Address: Calico Life Sciences, LLC, 1170 Veterans Blvd, South San Francisco, 94080, USA.

[6] FAS Informatics Group, Harvard University, Cambridge, MA 02138, USA.

.

ABSTRACT

While recent studies have uncovered dedicated neural pathways mediating the positive control of parenting, the regulation of infant-directed aggression and how it relates to adult-adult aggression is poorly understood. Here we show that *urocortin-3* (*Ucn3*)-expressing neurons in the hypothalamic perifornical area (PeFA^{Ucn3}) are activated during infant-directed attacks in males and females, but not other behaviors. Functional manipulations of PeFA^{Ucn3} neurons demonstrate the role of this population in the negative control of parenting in both sexes. PeFA^{Ucn3} neurons receive input from areas associated with vomeronasal sensing, stress, and parenting, and send projections to hypothalamic and limbic areas. Optogenetic activation of PeFA^{Ucn3} axon terminals in these regions triggers various aspects of infant-directed agonistic responses, such as neglect, repulsion and aggression. Thus, PeFA^{Ucn3} neurons emerge as a dedicated circuit component controlling infant-directed neglect and aggression, providing a new framework to understand the positive and negative regulation of parenting in health and disease.

INTRODUCTION

Mammals invest considerable resources to protect and nurture young offspring. However, under certain physiological and environmental conditions, animals neglect or attack young conspecifics. Specifically, males in some species kill unfamiliar infants to gain reproductive advantage (Hrdy, 1974; 1979; Parmigiani & Vom Saal, 1994), and females in many species are known to cull or neglect their young during stressful circumstances such as food shortage or high risk of predation (Svare, 1978; Heasley, 1983; Marsteller & Lynch, 1987; König, 1989; Lukas & Huchard, 2018). Notably, stress in humans of both sexes has been identified as a major risk factor for peripartum mental disorders and associated impairments in parent-infant interactions (Bloch *et al.*, 2003; Scarff, 2019; Hutchens & Kearney, 2020).

In species with biparental care, male's onset of parenting behavior and loss of infant mediated aggression typically coincide with the timing of birth of offspring following mating (vom Saal, 1985;

Tachikawa *et al.*, 2013; Wu *et al.*, 2014). This phenomenon of time-dependent parental care is observed in biparental mammals, as well as more widely throughout the animal kingdom, such as insects, fish, and birds (Elwood, 1994).

Recent studies have investigated the neural mechanisms underlying parental behavior and uncovered specific circuit nodes and neuronal populations mediating the positive control of parenting (Wu *et al.*, 2014; Marlin *et al.*, 2015; Scott *et al.*, 2015; Fang *et al.*, 2018; Kohl *et al.*, 2018; Stagkourakis *et al.*, 2020). However, the existence of a similar circuit organization to control infant-directed aggression and the relationship between such pathway and that of adult-mediated aggression have not yet been determined (Tachikawa *et al.*, 2013; Tsuneoka *et al.*, 2015; Amano *et al.*, 2017; Chen *et al.*, 2019; Sato *et al.*, 2020). Using induction of the immediate early gene (IEG) *c-fos* as a molecular readout of neuronal activation after interaction with pups, we found that *urocortin-3* (*Ucn3*)-expressing neurons in the perifornical area (PeFA^{Ucn3}) of the hypothalamus are activated during infant-directed attacks in male and female mice, but not during other forms of aggression. Inhibition of PeFA^{Ucn3} neurons in virgin males suppresses infant-directed aggression, while activation of these cells in virgin females disrupts parental behavior. We determined the input and output organization of PeFA^{Ucn3} neurons and showed that optogenetic activation of PeFA^{Ucn3} axon terminals in specific target regions, i. e ventromedial hypothalamus (VMH), ventral lateral septum (LSv) and amygdalohippocampal area (AHi), triggers different aspects of infant-directed agonistic responses, such as neglect, repulsion and aggression. Based on their function and connectivity, PeFA^{Ucn3} neurons help define a new brain pathway mediating the specific expression of infant-directed neglect and aggression. These findings provide new mechanistic insights into the control of opposite behaviors toward infants according to an animal's sex and physiological status.

RESULTS

Urocortin-3 expressing cells in the perifornical area are specifically activated during infant-directed aggression

To identify neuronal populations involved in infant-directed aggression, we monitored the induction of the immediate early gene (IEG) *c-fos* across brain regions involved in social behavior control, i.e., the hypothalamus and septal and amygdaloid nuclei, in infanticidal virgin males, fathers and mothers after interactions with pups (Figure 1A, B). Significantly more *c-fos*+ cells were identified in the medial bed nucleus of stria terminalis (BNSTm), the ventral lateral septum (LSv), and perifornical area (PeFA) of infanticidal males compared to mothers and fathers, with the most robust differences in *c-fos* expression between infanticidal and parental animals observed in the PeFA, a small nucleus between the fornix and the paraventricular hypothalamus (PVH) (Figure 1 A, B). By contrast, only rare *c-fos*+ cells were observed in the medial preoptic area (MPOA) of infanticidal males compared to mothers, as expected from previous studies (Wu *et al.*, 2014; Kohl *et al.*, 2017) (Figure 1 A, B).

Based on the abundant literature highlighting the critical role of hypothalamic nuclei in infant-adult interactions we focused our study on the role of the PeFA in infanticidal behavior and performed an expression analysis to characterize the identity of PeFA cells activated by infant-directed attacks. For this purpose, we visualized *c-fos* expression by *in situ* hybridization in tissue sections from virgin males after interactions with pups and performed laser capture microdissections of the corresponding *c-fos* + areas in adjacent sections left untreated, followed by gene expression analysis of this material (Figure 1C).

Expression analysis revealed 140 transcripts with significant differential expression between the *c-fos*+ area and the adjacent dorsolateral *c-fos* negative hypothalamic tissue. Among them, *vasopressin* (*Avp*) and *urocortin-3* (*Ucn3*) were the most up-regulated transcripts, followed by *oxytocin* (*Oxt*), *thyrotropin releasing hormone* (*Trh*), and *galanin* (*Gal*), each with a more than 2-fold change (log2) in gene expression relative to the dorsolateral *c-fos*-negative region (Figure 1D; $p < 0.001$, adjusted p value < 0.05). Phosphorylated-S6 ribosomal pulldown (Knight *et al.*,

2012) after pup-directed attack further confirmed the enrichment in *Ucn3* expression in neurons activated by infanticide (Figure 1—figure supplement 1a). In situ hybridization analysis showed that *Ucn3* expression is spatially restricted to the PeFA and is not expressed in the paraventricular nucleus nor in other surrounding brain areas (Figure 1E). This is in agreement with previous studies describing specific expression of *Ucn3* in the PeFA, as well as in few other brain regions such as the posterior bed nucleus of the stria terminalis (pBNST), the MPOA, the medial amygdala, and the nucleus ambiguus (Venihaki *et al.*, 2004; Wittmann *et al.*, 2009; Deussing *et al.*, 2010). Overall, *Ucn3* displayed the highest colocalization with *c-fos*+ cells after infanticide (55.3% *c-fos*+ cells co-express *Ucn3*) compared to *Avp* (7.5% *c-fos*+ cells co-express *Avp*) (Figure 1—figure supplement 1B). Significant expression overlap was also seen between *c-fos* and *Trh* (Figure 1—figure supplement 1B), consistent with a previous report of co-expression of *Ucn3* and *Trh* by large fractions of PeFA neurons (Wittmann *et al.*, 2009). By contrast, few neurons active during infanticide were marked by *Gal* (20.8%), a marker that is highly co-expressed with *c-fos* (42.8%), as detected by our microarray (Figure 1D) and pS6 data (Figure 1—figure supplement 1A, B), but that labels only a very small subset of PeFA neurons. Another candidate marker, *Oxt*, did not colocalize significantly with *c-fos* in mice that committed infanticide (Figure 1—figure supplement 1B), and may have been mistakenly identified due to its high level of expression in this region of the hypothalamus. Quantification of *Ucn3* and *c-fos* colocalization across the entire PeFA revealed that while *Ucn3*+ cells are found throughout the PeFA, *Ucn3*+/*c-fos*+ neurons identified after infant-directed attack are located primarily in the rostral half of the PeFA (Figure 1 E, F).

Next, we asked whether the activity of *Ucn3*+ PeFA neurons ($PeFA^{Ucn3}$) neurons was specifically associated with infant-directed agonistic interactions or was more generally increased by aggressive displays. We found that a significant number of PeFA neurons were activated by pup-directed attack in virgin males and females as well as by acute stress (Figure 1H; green dots). However, remarkably, when looking specifically at the *Ucn3*+ subpopulation in

PeFA, *c-fos* expression was only significantly induced in PeFA^{Ucn3} neurons after pup-directed attacks by virgin males compared to fresh bedding exposure. A trend was also observed in infanticidal virgin females, resulting from the analysis of 3 rare infanticidal mice seen out of a large group of otherwise non-aggressive virgin females. Strikingly, no *c-fos* induction was observed in PeFA^{Ucn3} neurons after other forms of aggression such as maternal defense, inter-male aggression and predation, nor by stress or feeding, suggesting a specific role of this population in infant-directed aggression (Figure 1 G, H; yellow bars). In addition, while *Ucn3*+ cells did not express *c-fos* in lactating females after exposure to pups, a non-statistically significant trend toward activation of *Ucn3*+ neurons in virgin females that either attacked or retrieved pups was observed, suggesting some engagement of this population in virgin states (Figure 1H; Figure 1—figure supplement 1E). No sex or state-dependent difference was observed in the number of PeFA^{Ucn3} neurons in virgin or mated males and females (Figure 1—figure supplement 1C), and most PeFA^{Ucn3} neurons expressed the vesicular glutamate transporter 2 (*Vglut2*, or *Slc17a6;* 91.3%±1.2%) suggesting an excitatory function (Figure 1—figure supplement 1D).

We conclude from these data that pup-directed aggression, but no other forms of adult aggression or other behaviors, specifically activates excitatory *Ucn3*+ neurons of the rostral PeFA.

Inhibition of PeFA^{Ucn3} neuronal activity in virgin males blocks infanticide

To test if PeFA^{Ucn3} neuronal activity is required for the display of male infanticide, we used a conditional viral strategy to express the inhibitory opsin NpHR3.0, or yellow fluorescent protein (YFP), in PeFA^{Ucn3} neurons and implanted bilateral optical fibers above the PeFA of virgin males (Figure 2A, Figure 2—figure supplement 2). Before laser stimulation, control and NpHR3.0-injected males showed similarly high levels of pup-directed aggression with short latencies to attack (Figure 2B-D). By contrast, optogenetic inhibition of PeFA^{Ucn3} neurons led to a reduction

in the number of males displaying pup-directed attacks, an increase in attack latency and a decrease in the duration of aggressive displays toward pups (Figure 2B-D). Strikingly, the suppression of pup-directed aggression persisted – and even further increased – within the next 24h till at least the second "laser off "session, suggesting a prolonged effect of acute PeFA^{Ucn3} neuronal silencing ("OFF(2)" in Figure 2B-D). Males spent equivalent time investigating pups in all conditions and did not increase their parental behaviors within the test period (Figure 2 E, F). Furthermore, PeFA^{Ucn3} silencing did not affect motor activity and, importantly, did not reduce adult intruder-directed aggression (Figure 2G). These data suggest that PeFA^{Ucn3} neuron activity is involved in the regulation of pup-directed aggression but not pup investigation, motor control nor adult-mediated aggression.

Activation of PeFA^{Ucn3} neurons elicit infant-directed neglect in virgin females

To test if the activity of PeFA^{Ucn3} neurons is sufficient to trigger infant-directed agonistic interactions in females, we used conditional viruses to express the excitatory opsin Channelrhodopsin-2 (ChR2), or a control fluorophore, in PeFA^{Ucn3} neurons (Figure 3A, Figure 3—figure supplement 3A). Parenting experience strongly impacts subsequent interactions of virgin females with pups (Lonstein & De Vries, 2000; Okabe *et al.*, 2013) and indeed, sessions in mice injected with ChR2 in which the laser OFF condition was tested first --leading to an initial parenting bout-- led to irreversible parental behavior in all subsequent sessions (Figure 3—figure supplement 3B, C). Hence, all sessions were started with the laser ON condition in both experimental and control groups, followed by laser OFF in the second session, and back to laser ON in third session (see methods). As expected, control females improved their parenting from session to session, with more pups retrieved and with shorter latencies in each subsequent session (Figure 3B, C). By contrast, optogenetic stimulation of PeFA^{Ucn3} neurons reduced female parenting with fewer pups collected and with longer latencies in the third session compared to first (laser ON) and second (laser OFF) sessions (Figure 3B, C). Further, the duration of parental

behaviors, investigation bout length, and time spent in the nest with pups were significantly reduced in the third compared to earlier sessions (Figure 3C-E), and fewer females in the ChR2 group retrieved pups to the nest (Figure 3F). While the overall display of pup-directed aggression (duration of aggression and number of females displaying aggression) was not significantly increased (Figure 3G), a subset of females (n=3/15) showed tail-rattling locked to laser stimulation, an overt sign of aggression never observed in control females (Supplementary Video 1). Further, activation of PeFA^{Ucn3} neurons did not affect motor activity or intruder-directed aggression (Figure 3H). Consumption of appetitive food was slightly decreased with activation of PeFA^{Ucn3} neurons in ChR2 females (Figure 3—figure supplement 3D), in agreement with the previously reported anorexigenic effect of this neural population (Fekete *et al.*, 2007; Jamieson *et al.*, 2011). To validate the efficiency of ChR2-mediated excitation of PeFA^{Ucn3} neurons, we used *in vitro* slice electrophysiology and performed whole cell patch clamp recordings from mCherry positive PeFA^{Ucn3} neurons (Figure 3—figure supplement 3E) to test various stimulation paradigms (465 nm blue light pulses of 5-20 ms pulse width at 2-20 Hz, Figure 3—supplemental figure 3F-G).

To further confirm the effects of PeFA^{Ucn3} neuron activation and assess the effects of prolonged activation in virgin females, we injected a conditional virus expressing the excitatory chemogenetic effector hM3Dq into either Ucn3::Cre+ or control Cre- females, followed by administration of its ligand clozapine-*n*-oxide (CNO) (Figure 4 -figure supplement 4A). To test the efficacy of chemogenetic activation of Ucn3::Cre+ neurons, we used *in vitro* slice electrophysiology and performed whole cell patch recordings from PeFA^{Ucn3} neurons (Figure 4—figure supplement 4 C-E) labelled with mCherry (Ucn3::Cre male mice injected with pAAV-hSyn-DIO-hM3D(Gq)-mCherry). Bath application of 10 μM CNO resulted in significant increase in the firing rate of the PeFA^{Ucn3} neurons (Figure 4—figure supplement 4E, p= 0.0013 compared to baseline, Wilcoxon rank sum method).

In vivo chemogenetic activation of PeFA^{Ucn3} neurons led to a decrease in pup retrieval compared to control (Cre-) females (18% pups retrieved versus 70%, Fisher's exact test $p<0.0015$) (Figure 4B; Kolmogorov-Smirnoff test $p<0.001$). Further, fewer experimental females displayed parental behaviors compared to controls, and we observed a decrease in overall parental behavior, reduced time in the nest with pups, and reduced nest building (Figure 4C, D). Pup-directed aggression was observed in few females after activation of PeFA^{Ucn3} neurons, including infant-directed attack and aggressive carrying (Figure 4E; see Methods). In addition, despite diminished parenting, females with activated PeFA^{Ucn3} neurons investigated pups as much as control females, suggesting they were not avoidant (Figure 4E). Together, these data suggest that activation of PeFA^{Ucn3} neurons reduced parenting in virgin females, and in a few cases induced signs of aggression. Of note, pilot attempts to stimulate PeFA^{Ucn3} neurons in mothers and to inhibit PeFA^{Ucn3} neurons in fathers showed no behavioral effects, suggesting that mated animals were insensitive to these manipulations, which were thus not pursued further (see Methods).

PeFA^{Ucn3} neurons receive input from parenting and stress-associated cell populations

To identify monosynaptic inputs to PeFA^{Ucn3} neurons, we used conditional rabies virus mediated retrograde trans-synaptic tracing in adult virgin males and females (Wickersham *et al.*, 2007) (Figure 5A). Fifteen brain areas were identified as providing monosynaptic inputs to PeFA^{Ucn3} neurons, which, strikingly, all resided within the hypothalamus, lateral septum, and medial amygdala, with the highest fraction of inputs originating from PVH and MPOA (Figure 5B-D). In particular, the PVH contained the highest fractional inputs to PeFA^{Ucn3} neurons in both sexes, with a higher fraction in females (44.92%±8.1%) compared to males (22.95% ± 4.2%) (Figure 5D). Neuronal inputs originating from the PVH were diverse and included Avp (31.9% ± 11.1%), *Crh* (17.8% ± 7.1%) and Oxt (9.1% ± 2.1%) expressing cells, i.e. populations implicated in social and stress responses (Swanson & Sawchenko, 1980; Jezova *et al.*, 1995; Donaldson & Young, 2008; Insel, 2010). In the MPOA, which constituted the second major input area to PeFA^{Ucn3}

neurons, around half (48.02%) of PeFA^{Ucn3} monosynaptic input were *Gal*+ cells, a largely GABAergic neural population involved in the positive control of parenting (Wu *et al.*, 2014; Kohl *et al.*, 2018) (Figure 5 E, F). Thus, PeFA^{Ucn3} neurons are poised to collect information from vomeronasal and hypothalamic pathways associated with stress and social behavior control, including inhibitory input from parenting behavior circuits.

PeFA^{Ucn3} neurons project to areas involved in aggression and anxiety

Next, we visualized PeFA^{Ucn3} axons and presynaptic terminals by conditional viral expression of synaptophysin-eGFP and tdTomato (Figure 6A). All observed PeFA^{Ucn3} projections were within the hypothalamus and limbic areas, with the most densely labelled projections in AHi, LSv, PVH, and VMH (Figure 6B-D). No obvious sex differences were observed (Figure 6B-D).

To better understand the organization of PeFA^{Ucn3} neuronal projections, we performed pairwise injections of the fluorophore conjugated cholera toxin B subunit (CTB-A488 and CTB-A647) retrograde tracers (Figure 7 A, B). We focused on PeFA^{Ucn3} projections to LS, AHi, and VMH, based on their dense labelling and on the known functions of these target areas in stress and aggression (Slotnick *et al.*, 1973; Blanchard *et al.*, 1977; Albert & Chew, 1980; Kruk *et al.*, 1983; Canteras *et al.*, 1997; Lin *et al.*, 2011; Anthony *et al.*, 2014; Lee *et al.*, 2014). For each paired target injection, around 50-60% of PeFA^{Ucn3} neurons were labelled by both tracers (Figure 7C), suggesting that individual PeFA^{Ucn3} neurons project to multiple targets. To further determine the respective organization of these projections from the PeFA and their involvement in pup-directed aggression, we performed CTB-mediated retrograde tracing from LS, VMH and AHi individually and quantified the overlap between CTB labelling and C-fos expression in the PeFA of virgin males after infant-directed attack (Figure 7 D, E). C-fos labeling was found in PeFA neurons associated with each of the three major projections, with AHi-projecting C-fos+ cells preferably located in the rostral and medial subdivision of PeFA (Figure 7F, G).

Functional analysis reveals strongest connectivity between PeFA^{Ucn3} neurons and AHi

To assess the strength of the functional connectivity between PeFA ^{Ucn3} neurons and downstream targets, we used conditional AAVs to express ChR2 and mCherry in PeFA^{Ucn3} neurons (Figure 8 A-B). We performed whole-cell patch clamp recordings from putative post synaptic neurons in the three targeted areas: LS, VMH and AHi (Figure 8 A-B). Our data showed that PeFA^{Ucn3} neurons make functional connections with neurons in AHi with a mean evoked EPSC amplitude of 47.32±4.8 pA (4 out of 7 neurons), in LS with a mean evoked amplitude of 20.78±1.42 pA (7 out of 7 neurons) and in VMH with a mean evoked amplitude of 9.75±2.67 pA (2 out of 9 neurons) (Figure 8C-D). Based on the observed evoked EPSC amplitudes, the AHi appears to receive significantly stronger connections from PeFA^{Ucn3} (Figure 8D) than the other two areas tested ($p=2.55*10^{-7}$ for AHi to LS comparison and $p=2.73*10^{-8}$ AHi to VMH comparison, Wilcoxon rank sum test).

Next, we used a paired pulse stimulation protocol to estimate the probability of connectivity and probability of release from PeFA^{Ucn3} neurons to each of these 3 brain areas (Figure 8E). We found that PeFA^{Ucn3} projections to LS and AHi showed high probability of release (Figure 8E top and bottom), as evident from the significant depression to the paired pulse paradigm ($p=2.10*10^{-5}$ for AHi and $p=2.20*10^{-3}$ for LS for paired pulse depression, Wilcoxon rank sum test). By contrast, PeFA^{Ucn3} projections to VMH displayed weak probability of release ($p=4.3*10^{-2}$ for paired pulse depression, Wilcoxon rank sum test) as evidenced by lack of depression to the paired pulse paradigm (Figure 8E middle row).

These functional connectivity data demonstrates that PeFA^{Ucn3} projections to AHi make significantly stronger connections (Figure 8D) with higher probability of release (Figure 8E bottom) compared to PeFA^{Ucn3} projections to other brain areas (i.e. LH and VMH, Figure 8D and 8E top and middle). Together with our anatomical data, these results suggest that all major

projections are active during pup-directed attacks with preferential involvement of rostro-medial PeFA^{Ucn3} projections to AHi.

PeFA^{Ucn3} neuronal projections govern discrete aspects of infant-directed neglect and aggression

To test the respective functions of PeFA^{Ucn3} targets, we performed optogenetic activation of PeFA^{Ucn3} terminals in virgin females injected in the PeFA with a conditional virus expressing ChR2 and with optical fibers implanted bilaterally above each projection target (Figure 9). We initially focused on projections to VMH, based on the documented role of this area in the control of aggression (Kruk *et al.*, 1983; Lin *et al.*, 2011). Stimulation of PeFA^{Ucn3} to VMH projections reduced pup retrieval across sessions and shortened individual bouts of pup investigation (Figure 9B; Supplementary Video 2). However, it did not affect the overall number of parental females, nor the overall time engaged in parental interactions, latency to retrieve, time spent in the nest with pups, or pup grooming (Figure 9C-E). Further, we did not observe any pup-directed aggression (Figure 9F). Slice recordings (Figure 8) had indicated that both the probability and the strength of connectivity between PeFA^{Ucn3} and VMH neurons is low, perhaps in part explaining the weak behavioral manifestation of the selective activation of PeFA^{Ucn3} to VMH projections. Thus, PeFA^{Ucn3} to VMH projections inhibit sustained interactions with pups and pup retrieval but do not elicit aggression toward pups.

We next stimulated the PeFA^{Ucn3} to LS projections (Figure 9G) and found that this manipulation inhibited parental behavior in a significant fraction of females and reduced cumulative pup retrieval and pup grooming across the three sessions (Figure 9 H, I). Moreover, stimulation of PeFA^{Ucn3} to LS projections triggered instances of pup-directed aggression (such as aggressive handling and biting) in 30% of females, although the overall time displaying aggression remained negligible (Figure 9J). PeFA^{Ucn3} to LS stimulation had no significant effect on time

spent in the nest with pups, pup investigation, overall parenting time and latency to retrieve (Figure 9K, L). In a subset of females (n = 2/10), PeFA^{Ucn3} to LS stimulation led to an escape response, which was never observed in other manipulations (Supplementary Video 3). Together, these results suggest that PeFA^{Ucn3} to LS projections inhibit parenting and mediate signs of repulsion and aggression.

Slice recordings revealed strong synaptic connectivity between PeFA^{Ucn3} projections and AHi neurons (Figure 8), suggesting that the PeFA^{Ucn3} to AHi projection may have a strong impact on pup-directed behaviors. Indeed, when we examined the function of PeFA^{Ucn3} to AHi projections (Figure 9M), we found that 55% of females displayed infant-directed aggression such as biting and aggressive carrying of pups without completing retrieval, in a manner similar to the stereotyped infanticidal behaviors observed in males, with increased time displaying aggression (Figure 9N, Supplementary Video 4). Additionally, PeFA^{Ucn3} to AHi stimulation dramatically reduced cumulative pup retrieval over the course of three sessions, time spent in the nest with pups, number of parental females and time spent pup-grooming (Figure 9 O, P) with no effect on retrieval latency, pup investigation bout length and time spent parenting (Figure 9 Q, R). Thus, stimulation of PeFA^{Ucn3} to AHi projections strongly increased the expression of infant-directed aggression and suppressed the expression of parental behavior.

In control experiments we found that stimulation of PeFA^{Ucn3} projections to VMH, LS and AHi did not impact locomotion, appetitive feeding, or conspecific aggression (Figure 9—figure supplement 9A-J).

Altogether, these data suggest that various aspects and degrees of infant-directed neglect and aggression are mediated across PeFA^{Ucn3} projections, with PeFA^{Ucn3} to VMH projections suppressing pup investigation, PeFA^{Ucn3} to LS projections mediating reduced pup handling and low-level aggression, and PeFA^{Ucn3} to AHi projections inducing stereotyped displays of pup-directed aggression (Figure 10).

Discussion

The last few decades have seen considerable progress in the use of experimental model systems to identify the neural basis of parental behavior (Noirot, 1972; Fleming & Rosenblatt, 1974a; vom Saal, 1985; Lonstein & De Vries, 2000; Dulac *et al.*, 2014; Wu *et al.*, 2014; Marlin *et al.*, 2015; Scott *et al.*, 2015; Kohl *et al.*, 2017; Kohl *et al.*, 2018; Numan, 2020; Stagkourakis *et al.*, 2020). These studies have uncovered critical sensory cues underlying parent-infant interactions, as well as brain circuits underlying specific nurturing displays in males and females (Dulac *et al.*, 2014; Wu *et al.*, 2014; Marlin *et al.*, 2015; Scott *et al.*, 2015; Kohl *et al.*, 2017; Kohl *et al.*, 2018)(Yoshihara *et al.*, 2021). By contrast, the neural control of infant-directed aggression remains less understood. Initially interpreted as a pathological behavior, Sarah Hrdy's pioneering work in langurs, as well as work in other mammalian species, instead put forward infanticide as an adaptive behavior that enables males to gain advantage over rivals, and females to adapt reproduction to adverse circumstances (Hrdy, 1974; 1979). Although a number of brain areas have been described that negatively affect parental behavior (Fleming & Rosenblatt, 1974a; b; Fleming *et al.*, 1980; Gammie & Nelson, 2001; Amano *et al.*, 2017; Isogai *et al.*, 2018), the existence of a dedicated neural circuitry controlling infant-directed agonistic interactions, including infanticide, had not yet been explored.

In the present study, we demonstrate that PeFA^{Ucn3} neurons are specifically activated by pup-directed aggression in males and females, but not by feeding, adult conspecific aggression, or acute restraint stress. Through functional manipulations we find that PeFA^{Ucn3} neurons are required for infant-directed aggression in males. In females, direct activation of PeFA^{Ucn3} neuronal projections to AHi elicited overt aggression toward pups while somatic activation of PeFA^{Ucn3} neurons strongly reduced maternal behavior including pup retrieval, time in the nest and overall parenting time but did not cause widespread aggressive displays, except tail rattling in few animals. Our input analysis of PeFA^{Ucn3} neurons provided us with useful information to

understand the different outcomes obtained by manipulation of PeFA neurons in males and females. Indeed, our study identified MPOA^{Gal} neurons, an inhibitory neuronal population driving the positive control of parenting (Wu et al., 2014; Kohl et al., 2018) as providing major inputs to PeFA^{Ucn3} neurons. MPOA^{Gal} neurons were also shown to share common targets with PeFA^{Ucn3} neurons, such as AHi, LS and VMH (Kohl et al., 2018). Activation of MPOA^{Gal} neurons has been shown to robustly, reversibly, and acutely enhance parental behavior in virgin females and fathers and to suppress ongoing infant-directed aggression in virgin males (Wu et al., 2014; Kohl et al., 2018). In our experiments, MPOA^{Gal} neurons are likely to be strongly activated in females exposed to pups, thus presumably exerting their putative inhibitory role on PeFA^{Ucn3} neurons and their projections, therefore occluding the full expression of pup-directed agonistic behavior following artificial activation of PeFA^{Ucn3} neurons in females but less so when more direct activation is provided to PeFA^{Ucn3} neuronal projections to AHi. Further investigation of PeFA^{Ucn3} neuron function while MPOA^{Gal} neuron activity is inhibited will be necessary to address this hypothesis.

Inhibition of PeFA^{Ucn3} neurons has a robust effect to suppress ongoing infant-directed attack behavior, but unlike MPOA^{Gal} neuron stimulation, this effect appears long-lasting and does not reverse in the short term. We interpret this result as indicating that suppression of PeFA^{Ucn3} neuron activity induces downstream circuit plasticity that favors the stable expression of parenting and inhibition of pup-mediated aggression. Indeed, we attempted to activate PeFA^{Ucn3} neurons in mothers and fathers in pilot experiments and were unable to observe increased neglect or aggression, suggesting that PeFA^{Ucn3} neuron activation cannot overcome the MPOA^{Gal} circuit activity in parental animals.

Previous studies have shown that electrical stimulation of the PeFA leads to a so-called ‘hypothalamic rage response’ comprising typical aggressive displays including piloerection, teeth baring, and bite attacks (Slotnick *et al.*, 1973; Kruk *et al.*, 1983; Canteras *et al.*, 1997).

Indeed, we observe *c-fos*+ neurons in the PVH and PeFA of males and females displaying conspecific aggression, but these neurons are *Ucn3*-negative, suggesting that distinct PeFA populations mediate aggression toward either adults or infants. In addition, previous studies have implicated *Ucn3* in the PeFA in the regulation of social recognition, stress responsivity, and more recently risk assessment (Venihaki *et al.*, 2004; Deussing *et al.*, 2010; Kuperman *et al.*, 2010; Jamieson *et al.*, 2011; Horii-Hayashi *et al.*, 2021). However, our experiments with targeted inhibition or stimulation of PeFA^{Ucn3} neurons specifically affected parental behavior with no impact on adult social behavior, indicating that PeFA^{Ucn3} neurons may be specifically tuned to social cues from infants and/or juveniles rather than adult conspecifics.

Specific tuning of these neurons to social cues is supported by our finding that input areas to PeFA^{Ucn3} neurons include the MPOA, MeA, and PVH, known to be essential for integration of social cues sensed by the vomeronasal system which has been well-established as a crucial pathway for infanticide (Tachikawa *et al.*, 2013; Wu *et al.*, 2014). MPOA^{Gal} neurons directly send input to PeFA^{Ucn3} neurons, suggesting a direct relationship between this well-established hub for pro-parental behavior and the putative infant-directed aggression neuron population described here. Inputs from PVH largely express *Avp* and *Crh*, and *Avp*-expressing PVH neurons have previously been implicated in male-typical social behavior (Donaldson & Young, 2008; Insel, 2010), while *Crh*-expressing PVH neurons are essential mediators of the physiological stress response (Vale *et al.*, 1981; Ulrich-Lai & Herman, 2009).

Previously identified hypothalamic neuronal populations critical for feeding (for example, *Agrp*-expressing neurons in the arcuate nucleus) and parenting (MPOA^{Gal} neurons) have been shown to be organized in distinct pools, each largely projecting to a distinct downstream area (Betley *et al.*, 2013; Kohl *et al.*, 2018). In contrast, individual PeFA^{Ucn3} neurons project to multiple targets, in a similar manner to VMH neurons extending collaterals to downstream defensive circuits (Wang *et al.*, 2015). Interestingly, the three major PeFA^{Ucn3} target areas VMH, LS and AHi convey overlapping but distinct aspects and degrees of infant-directed neglect and

aggression. Our recording data suggests that PeFA^{Ucn3} projections make direct excitatory functional connections with the neuronal populations of LS, VMH and AHi. Among these areas, PeFA^{Ucn3} projections to AHi showed particularly strong connectivity and high probability of release, and when stimulated lead to overt pup-directed attack behaviors. By contrast, weaker connectivity was identified between PeFA^{Ucn3} and LS and VMH neurons, which may in part explain the less robust behavioral manifestations of selective activation of PeFA^{Ucn3} projections to LS and VMH (Wittmann *et al.*, 2009; Chen *et al.*, 2011; Battagello *et al.*, 2017).

Taking the connectivity strength and functional behavior results altogether, our data suggest that each projection may participate in different aspects and degrees of agonistic responses to pups. Based on the role of VMH in conspecific aggression (Lin *et al.*, 2011; Yang *et al.*, 2013), we hypothesized a role for PeFA^{Ucn3} to VMH projection in pup-directed attack. However, we found instead that this projection regulates pup investigation. The PeFA^{Ucn3} to LS projections also led to sustained reductions in pup interactions, a finding that is consistent with a recent study showing that LS neurons expressing corticotrophin-releasing factor receptor 2 (CRFR2), the high-affinity receptor for *Ucn3*, may control persistent anxiety behavior (Anthony *et al.*, 2014) and, in addition, led to incidences of pup-directed aggression. The function of the AHi is not well understood, although recent data suggest it may send sexually-dimorphic projections to MPOA^{Gal} neurons essential for parenting (Kohl *et al.*, 2018), while projections from the AHi to the MPOA have recently been shown to modulate infant-directed behavior (Sato *et al.*, 2020). We noticed that the AHi-projecting neurons that are active during infanticide were located predominantly in the rostral PeFA, as were the majority of PeFA^{Ucn3} neurons associated with infanticide. Thus, we propose that the pattern of activation within subsets of PeFA^{Ucn3} neurons defined by their projection targets correlates with the degree of anti-parental behavior displayed by the individual, from neglect and avoidance, to genuine pup directed attack.

In turn, the roles of distinct PeFA^{Ucn3} neuronal projections in the expression of pup-directed behavior may explain the different behavior outcomes we observed between somatic

and projection stimulation of PeFA^{Ucn3} cells. Following PeFA^{Ucn3} somatic optogenetic stimulation, we observed neglect and some rare instances of aggression toward pups. Stimulation of PeFA^{Ucn3} to lateral septum projections led to pup avoidance, a more pronounced phenotype than what was observed in the somatic stimulation group. Following stimulation of PeFA^{Ucn3} to ventromedial hypothalamus projections, we observed pup neglect that was fairly similar to behavior observed with somatic stimulation. By contrast, stimulation of PeFA^{Ucn3} to AHi projections led to overt aggressive behavior in about half the females tested, a much more pronounced response than the soma stimulation group. Thus, direct stimulation of a specific projection may be more efficient in triggering behaviors directly related to the function of the target region. For example, LS is known to have a role in persistent anxiety-like phenotypes and indeed, stimulation of this projection elicits extreme pup avoidance. Similarly, the AHi has recently been associated with infant-directed aggression (Sato *et al.*, 2020), supporting our hypothesis that this projection target is preferentially involved in pup attack behavior.

Additionally, there is a strong level of connectivity between pro-parental MPOA^{Gal} and anti-parental PeFA^{Ucn3} -associated circuits. Indeed, MPOA^{Gal} and PeFA^{Ucn} neurons have been found to project to many of the same target regions, including the VMH and LS (Kohl *et al.*, 2018), and we found that about half of the monosynaptic inputs to the PeFA^{Ucn3} cells originate from MPOA^{Gal} neurons (Figure 5). Thus, the strength of MPOA^{Gal} inhibitory tone in parental animal is likely to strongly affect the behavioral outcomes observed after somatic versus projection stimulation of PeFA^{Ucn3} neurons.

Parental behavior, and by extension infant-directed aggression, is highly regulated by context and previous social experience. Previous studies have shown that females with repeated exposure to pups will become more parental over time (Lonstein & De Vries, 2000) . Our experiments with virgin females also showed a similar strong effect of pup exposure on subsequent infant-directed behavior. We observed that males allowed to interact with pups during suppression of PeFA^{Ucn3} neurons displayed long lasting reduced aggression toward

pups, and that activation of PeFA^{Ucn3} neurons in females induced prolonged reduction in parenting. These results stand in contrast to the effects of stimulation of the MPOA^{Gal} neurons which confers rapid, reversible facilitation of parental behavior (Wu *et al.*, 2014; Kohl *et al.*, 2018). Together, these data suggest that PeFA^{Ucn3} neurons may undergo significant plasticity leading to long lasting functional changes and may induce enduring changes in downstream parental circuitry.

The functional characterization of the PeFA^{Ucn3} neurons and their major projection targets enabled us to uncover how this neural population plays a role in regulating pup-directed neglect and aggression, thus revealing a pathway that is distinct from the brain control of adult-directed aggressive responses. This may have implications for the understanding of infant-directed behavior in many taxa as hypothalamic structures and peptides are highly conserved across species. We found that specific projections control aspects of anti-parental behavior such as the duration of pup investigation, repulsion, as well as stereotyped displays of pup-directed agonistic behavior. The discovery of a dedicated circuit node for pup-directed aggression further supports the notion that this behavior might have adaptive advantages in the wild. This study reveals a novel neural substrate for understanding how parental behavior is modulated at a circuit level and opens new avenues for studying the context- and physiological-state dependent expression of parenting in health and disease.

Data and code availability statement

The data and code that support the findings of this study are available in a public repository (see Methods).

Ethical statement

All animal experiments were approved by the Harvard University Institutional Animal Care and Use Committee. All experiments were performed in compliance with our Harvard University IACUC approved protocols.

Acknowledgements

We thank S. Sullivan for help with behavior scoring and mouse husbandry, and R. Hellmiss at MCB Graphics for work on illustrations. We thank members of the Dulac lab for comments on the manuscript, A. Leonard, E. Owolo, and L. Moussalime for assistance with data collection. This work was supported by a NIH K99 and R00 Award (K99HD085188, R00HD085188) and a NARSAD Young Investigator award to A.E.A., a Human Frontier Long-Term Fellowship, a European Molecular Biology Organization Long-Term Fellowship (ALTF 1008-2014) and a Sir Henry Wellcome Fellowship from the Wellcome Trust to J.K., a NIH K99 Award (K99HD092542) to D.J.B.M, a Howard Hughes Gilliam Fellowship for Advanced Study to B.M.B., and NIH grant 1R01HD082131-01A1 to C.D. C. D. is an investigator of the Howard Hughes Medical Institute.

Author Contributions

A.E.A. and C.D. conceived and designed the study. A.E.A. performed and analyzed laser capture and microarray, in situ hybridization experiments, pS6 pulldown, optogenetic, chemogenetic, and tracing experiments. Z. Wu participated in study design, laser capture strategy, in situ hybridization experiments, and technical details of optogenetic experiments. J.K. participated in optogenetic experiments, V.K performed slice electrophysiology, D.B. helped with pS6 pulldowns, N.D.R. and M.T. with statistical analysis, B.M.R. with data collection and quantification, I.C. and V.S. with behavior quantification. A.E.A, Z. W., J.K., V. K., D.B., N.D.R., and C.D. analyzed and interpreted results. A.E.A. and C.D. wrote the manuscript with input from all authors.

Competing Interests

The authors declare no competing financial interests.

FIGURES

METHODS

Animals

Mice were maintained on a 12h:12h dark light cycle with access to food and water ad libitum. All experiments were performed in accordance with NIH guidelines and approved by the Harvard University Institutional Animal Care and Use Committee (IACUC).

C57BL/6J mice as well as mice on a mixed C57BL/6J x 129/Sv background were used for the molecular identification of activated PeFA neurons.

The Ucn3::Cre BAC transgenic line (STOCK Tg(Ucn3-cre) KF43Gsat/Mmcd 032078-UCD) was resuscitated from sperm provided by MMRRC. This line was generated by inserting a Cre-recombinase cassette followed by a polyadenylation sequence into a BAC clone at the initiating ATG codon of the first coding exon of the Ucn3 gene. Sperm from the mixed B6/FVB male was introduced into oocytes from a B6/FVB female and the founding Cre+ animals were backcrossed to C57BL/6J. Mice from the F1 and F2 generations were used in experiments.

Behavior assays

Mice were individually housed for at least 1 week prior to testing. Experiments were conducted during the dark phase under dim red light. Tests were recorded by Geovision surveillance system or by Microsoft LifeCam HD-5000 and behaviors were scored by an observed blind to experimental condition using Observer XT11 Software or Ethovision XT 8.0 (Noldus Information Technology). Animals were tested for a single behavior per session with at least 24 hours between sessions.

Parental behavior

Parental behavior tests were conducted in the mouse's home cage as previously described (Wu *et al.*, 2014; Kohl *et al.*, 2018). Mice were habituated to the testing environment for 10 minutes. One to two C57BL6/J pups 1-4 days old were presented in the cage in the opposite corner to the

nest. Test sessions began when the mouse first closely investigated a pup (touched the pup with its snout) and lasted for 5-15 minutes. In the event that the mouse became aggressive by biting and wounding the pup, the session was immediately halted and the pup was euthanized. The following behaviors were quantified: latency to retrieve, sniffing (close contact), grooming (handling with forepaws and licking), nest building, time spent in the nest, crouching, latency to attack (latency to bite and wound), aggression (roughly handling, aggressively grooming, aggressive carrying with no retrieval), and tail rattling. A 'parenting behavior' index was calculated as the sum of duration of sniffing, grooming, nest building, time spent in the nest, and crouching. Mice were categorized as 'parental' if they showed pup-retrieval behavior and 'non-parental' if they did not retrieve pups. Mice were categorized as 'aggressive' if they showed bite attacks, tail rattling, aggressive pup carrying or aggressive pup-grooming and 'non-aggressive' if they did not display any of these behaviors. Optogenetic experiments were limited to 5 minutes as previously performed for infanticidal testing, thus limiting the ability to score male retrieving behavior which is typically displayed between 4 and 7 minutes(Wu *et al.*, 2014; Kohl *et al.*, 2018).

Conspecific aggression

Conspecific aggression assays were performed as previously described[30]. Briefly, castrated males were swabbed with ~40 µL of urine from an intact male and introduced into the home cage of the test mouse for 5 minutes (session started at first close contact).

Locomotor behavior

Locomotor behavior assays were performed in a 36 x 25 cm empty cage. Velocity and distance moved were tracked for 5 minutes.

Feeding behavior

Feeding behavior was assessed by introducing a small piece of palatable food (chocolate chip cookie) into the far corner of a mouse's home cage. Session started when mouse approached the food and behavior was recorded for 5 minutes. Parameters rated were duration sniffing and eating the cookie.

Fluorescence in situ hybridization

Fluorescence *in situ* hybridization (FISH) was performed as previously described (Isogai *et al.*, 2011; Wu *et al.*, 2014). Briefly, fresh brain tissue was collected from animals housed in their home cage or 35 min after the start of the behavior tests for immediate early gene (c-fos) studies. Only animals that engaged in a particular behavior were used. Brains were embedded in OCT (Tissue-Tek) and frozen with dry ice. 20 µm cryosections were used for mRNA in situ. Adjacent sections from each brain were collected over replicate slides to stain with multiple probes. The staining procedure is as previously described(Isogai *et al.*, 2011; Wu *et al.*, 2014). Complementary DNA of *c-fos, ucn3, gal, crf, trh, pdyn, cart, sst, oxt, penk, avp, and yfp* were cloned in approximately 800-1200 base pairs (when possible) segments into pCRII-TOPO vector (Invitrogen). Antisense complementary RNA (cRNA) probes were synthesized with T7 or Sp6 (Promega) and labelled with digoxigenin (DIG; Roche) or fluorescein (FITC, Roche). Where necessary, a cocktail of 2 probes was generated covering different segments of the target sequence to increase signal to noise ratio.

Probe hybridization was performed with 0.5-1.0 ng/l cRNA probes in an oven at 68° C. Probes were detected by horseradish peroxidase (POD)-conjugated antibodies (anti-FITC-POD at 1/250 dilution, Roche; anti-DIG-POD at 1/500 dilution, Roche). Signals were amplified by biotin-conjugated tyramide (PerkinElmer) and visualized with Alexa Fluor-488-conjugated streptavidin or Alexa Fluor 568-conjugated streptavidin (Invitrogen), or directly visualized with TSA plus cyanine 3 system, TSA plus cyanine 5 system, or TSA plus Fluorescein system (PerkinElmer). Slides were mouted with Vectashield with 4',6-diamidino-2-phenylindole (DAPI, Vector Labs).

Laser-capture microscopy and microarray analysis

Males were sacrificed 35 minutes after onset of attacking behavior for peak c-fos expression and fresh brain tissue was frozen in OCT. 20µm sections with alignment holes punched into the tissue by a glass pipet were prepared in a series with every other section aimed for *in situ* hybridization and collected on superfrost plus slides and the other for laser capture

microdissection and collected on PEN coated membrane slides (Leica). Double fluorescence *in situ* hybridization (FISH) for *c-fos* and *oxytocin* was performed as previously described (Isogai *et al.*, 2011; Wu *et al.*, 2014). Sections prepared for laser-capture were dehydrated and stained in a 50% ethanol solution containing cresyl violet. Using a Zeiss PALM microscope, slides from adjacent FISH and laser-capture sections are aligned via tissue pinches using PALM Software (Zeiss). After alignment, tissue from the area containing *c-fos*+, oxytocin+ cells, and an outside region were identified from FISH sections and collected from fresh laser sections by laser capture. For each region, tissue from 6 brains were pooled to prepare total RNA (RNEasy micro kit, Qiagen) for reverse transcription and amplification to cDNA (Ovation Pico WTA kit, Nugen). Three replicates of cDNA (n=18 total brain samples; 6 pooled per replicate) were prepared for hybridization to the Affymetrix Exon ST 1.0 array as described by the manufacturer. The mouse Affymetrix Exon 1.0 ST array was preprocessed by Bioconductor packages oligo (Carvalho & Irizarry, 2010) and limma (Ritchie *et al.*, 2015). Briefly, the raw CEL files were read in to R by read.celfiles function and normalized by rma algorithm (Irizarry *et al.*, 2003). Exon level expressions were summarized into transcript level and the probes were annotated by the moex10sttranscriptcluster.db bioconductor package (MacDonald, JW: moex10sttranscriptcluster.db: Affymetrix moex10 annotation data (chip moex10sttranscriptcluster). R package version 8.7.0). Differential gene expression was carried out by limma using limFit, eBayes and Toptable functions (Phipson *et al.*, 2016). Volcano plot was made by R from the toptable and using pvalue of 0.001 and absolute logFC >= 2 as a cutoff. Data are available on GEO (Accession: GSE161507) and the analysis code can be found at https://gitlab.com/dulaclab/ucn3_neuron_microarray.

pS6 pulldowns and RNAseq analysis

Adult male mice were habituated in their home cages to a testing room for 4 hours. Males were then either presented with a 1-4 day old C57BL/6J pup or no stimulus and allowed to interact for 10 minutes, after which time behavior was recorded and the pup was removed. Sixty minutes after stimulus presentation, males were sacrificed and a punch (1 mm diameter) was collected from a 2mm thick brain slice containing the perifornical area, the paraventricular nucleus, and part of the anterior hypothalamus. The tissue was processed for pS6 immunoprecipitation as described previously (Knight et al, 2012). Briefly, punches were held in (ice-cold homogenization buffer (10mM HEPES, 150mM KCl, 5mM MgCl2 and containing 1X phosphatase inhibitor cocktail, 1X Calyculin. Protease inhibitor cocktail (EDTA free), 250ug/ml Cycloheximide and 2.5ul/ml Rnasin) and 10 punches were pooled per sample, with 3 biological replicates taken from infanticidal and naïve groups. Tissue was homogenized, centrifuged for 10 minutes at 2000 g, subjected to treatment with 0.7% NP40 and 20mM DHPC and centrifuged for 10 minutes at (20,000rcf) at 4° C to obtain the supernatant containing the input fraction. A (10 µL sample) of the input was kept for sequencing and the remaining input fraction was incubated with Protein A Dynabeads (Invitrogen) conjugated to pS6 antibody (Life Technologies 44923G) at a concentration of around 4 µg/IP for 10 minutes at 4° C. Beads were collected on a magnet and washed in 0.15M KCl wash buffer, then associated RNAs were lysed into RLT buffer and RNA was isolated using the RNAeasy Micro kit (Qiagen) according to manufacturer's instructions. RNA was checked for quality and quantity on an Agilent tape station. High quality samples from matched input and IP fractions were prepared using the (Low-input Library Prep kit (Clontech). Sequenced reads were mapped with STAR aligner (Dobin *et al.*, 2013), version 2.5.3a, to the mm10 reference mouse genome and the Gencode vM12 primary assembly annotation(Mudge & Harrow, 2015), to which non-redundant UCSC transcripts were added, using the two-round mapping approach. This means that following a first mapping round of each library, the splice-junction coordinates reported by STAR, across all libraries, are fed as input to the second round of mapping. The parameters used in both mapping rounds are: outSAMprimaryFlag

="AllBestScore", outFilterMultimapNmax="10", outFilterMismatchNoverLmax="0.05", outFilterIntronMotifs="RemoveNoncanonical". Following read mapping, transcript and gene expression levels were estimated using MMSEQ (Turro *et al.*, 2011). Following that transcripts and genes which cannot be distinguished according to the read data were collapsed using the mmcollapse utility of MMDIFF (Turro *et al.*, 2014), and the Fragments Per Killobase Million (FPKM) expression units were converted to natural logarithm of Transcript Per Million (TPM) units since the latter were shown to be less biased and more interpretable (Wagner *et al.*, 2012). In order to test for differential gene activation between the infanticidal males and naïve males, we used a Bayesian regression model (Perez *et al.*, 2015). We defined the response (for each transcript or gene) as the difference between means of the posterior TPMs of the IP and input samples (i.e., paired according to the tissue punches from which they were obtained). The uncertainty in the response was computed as square root of the sum of the variances of the posterior TPMs of the IP and input samples divided by the number of posterior samples (1,000). The categorical factor for which we estimated the effect was defined as the behavior of the animal, meaning infanticidal and naïve, where naïve was defined as baseline. Hence, our Bayesian regression model estimates the posterior probability of the natural logarithm of the ratio between infanticidal IP TPMs divided by input TPMs and naive IP TPMs divided by input TPMs being different from zero. In order to define a cutoff of this posterior probability, above which we consider the activation (i.e. effect size) significant, we searched for a right mode in the distributions of posterior probabilities across all transcripts and genes (separately for each), and placed the cutoff at the local minima that separates the right mode from the left mode, which represents transcripts and genes for which the likelihood of differential gene activation is very weak and hence their posterior probability is dominated by the prior (Figure 1—Supplement 1A)). Data are available at GEO (Accession: GSE161552) and analysis code is available on Github (https://gitlab.com/dulaclab/ucn3_neuron_microarray/-/tree/master/braimSourceCode/braim.R).

Optogenetics

Ucn3::Cre mice 8-12 weeks old were used for these experiments. Pilot experiments and our previous observations indicated that mated parents were insensitive to manipulations aimed at reducing parental behaviors, so we used virgin males and females in order to maximize our opportunity to see decrements in parenting. Virgin males were prescreened for infanticidal behavior. We injected 200 nL of AAV1/DIO-hChR2-eYFP for activation or AAV1/FLEx-NpHR3.0-eYFP for inhibition (or AAV1/FLEx-YFP or AAV1/FLEx-tdTomato as control virus) bilaterally into the perifornical area (AP -0.6, ML ±0.3, DV -4.2). Mice recovered for 1-2 weeks and in a second surgery a dual fiber optic cannula (300 µm, 0.22 NA, Doric Lenses) was implanted 0.5 mm above the target area and affixed to the skull using dental cement. Cannula positions were as follows: PeFA = AP -0.6mm, ML ± 0.5mm, DV -3.7mm; LS = AP 0.3mm ML ± 0.5mm DV -3.2mm; VMH= AP -1.6 ML ± 0.5mm DV -5.2; AHi = AP -2.3mm, ML ± 2.5mm, DV -4.7mm. Mice recovered for an additional week prior to the start of behavioral testing. In pilot studies we found that order of testing impacted parental behavior results, so rather than randomizing test order, we alternated laser on and off conditions in the same order for both control and manipulated mice. For locomotion, feeding, and conspecific aggression tests, we randomized the order of laser on/off presentation. On test days, the fiber implant was connected to an optical fiber with commutator connected to either a 473 nm laser (150 mW, Laserglow Technologies), or a 460 nm LED (50W, Prizmatix) for ChR2 stimulation, or to a 589 nm laser (300mW, OptoEngine) for NpHR3.0 inhibition. Behavior tests were 5 minutes in duration for each condition and behavior category. For parental behavior assays with ChR2, the 473 nm laser or 460 nm LED was triggered in 20ms pulses at 20 Hz for 2 seconds when the mouse contacted the pup with its snout, and the order of laser sessions was on first, off second, on third. For locomotor experiments with ChR2 activation, the laser was triggered (20ms, 20 Hz, 2 seconds) every 10 seconds to approximately equivalent duration as the time laser was on during the parental sessions, and this stimulation pattern was selected based on previous studies and pilot data (Wu *et al.*, 2014; Kohl *et al.*, 2018). For cookie

experiments with activation, the laser was triggered when the mouse contacted the cookie. For conspecific aggression experiments with activation, the laser was triggered when the test mouse made close contact with the intruder mouse. The power exiting the fiber tip was 5mW, which translates to ~2 mW/mm^2 at the target region (calculator provided by Deissertoth lab at http://www.stanford.edu/group/dlab/cgi-bin/graph/chart.php). For all behavior assays with NpHR3.0, the 589 nm laser was illuminated (20 ms, 50 Hz) throughout the duration of the 5 minute session at a power of 15 mW, or ~8.4 mW/mm^2. For parenting sessions with inhibition, the order of laser sessions was off first, on second, off third.

Chemogenetics

Ucn3::Cre virgin female mice (or Cre negative littermates as controls) 8-12 weeks old were used for these experiments. We injected 200 nL of AAV1/DIO-HM3Dq virus bilaterally into the PeFA (AP -0.6mm, ±ML 0.3mm, DV -4.2mm). Mice recovered for two weeks prior to behavior testing. Cre positive and Cre negative females were administered 0.3mg/kg clozapine-n-oxide dissolved in saline intraperitoneally and habituated to the testing environment for 30 minutes. Females were presented two C57BL6/J pups in the corner of their homecage opposite the nest and parental behaviors were recorded for 15 minutes.

Anterograde tracing

AAV2.1-FLEX-tdTomato virus (UPenn Vector Core) and AAV2.1-FLEX-synaptophysin-eGFP virus (plasmid gift of Dr. Silvia Arber; custom virus prep, UNC Vector Core) were mixed at a ratio of 1:2 and stereotaxically injected unilaterally into the PeFA (Bregma coordinates AP: -0.6mm; ML: -0.3mm; DV: -4.2mm) using a Drummond Nanoject II (180 nL to cover entire structure) into adult virgin male (n=3) and female (n=3) Ucn3-cre mice. After 2 weeks, mice were transcardially perfused with 4% paraformaldehyde. Tissue was cryoprotected (30% sucrose) and serial sections were prepared on a freezing microtome (60 µm). Every third section (covering from the prefrontal cortex through the cerebellum) was immunostained using Anti-GFP antibody (described in immunohistochemistry methods), mounted to superfrost plus slides, coverslipped

with Vectashield plus DAPI and imaged at 10X magnification using the AxioScan (Zeiss). Synaptic densities were quantified by ImageJ software after background subtraction and a density ratio was prepared by dividing by the density at the injection site which was normalized to 100%. Density ratio was compared across brain regions by One-way ANOVA followed by Dunnett's test for multiple comparisons and sexual dimorphisms compared using a two-tailed t-test.

Retrograde tracing with CTB

Retrograde tracing was performed in either Ucn3::Cre males aged 8-12 weeks injected into the PeFA bilaterally with AAV1/FLEx-BFP allowed to recover for 10 days, or into C57BL6/J males aged 8 weeks prescreened for infanticide. In Ucn3::Cre males, pairwise injections of 80 nL of 0.5% (wt/vol) fluorescently labeled cholera toxin B subunit (CTB-488, ThermoFisher C22841, CTB-647, ThermoFisher C34788). In C57BL6/J mice, only CTB-488 was injected. After 7 days, Ucn3::Cre mice were transcardially perfused and brains were postfixed overnight, cryoprotected in 30% sucrose overnight, and 60 µM sections were prepared on a sliding microtome. Sections were imaged at 10X (Axioscan, Zeiss) and the fraction of BFP+ cells double-labeled with CTB-488 and CTB-647 was quantified. In control experiments, a 1:1 mixture of CTB-488 and CTB-647 was injected into the LS (AP +0.4mm; ML +0.5 mm; DV -3.7mm) and AHi (AP -2.3mm; ML +2.5mm; DV -4.9mm). In C57BL6/J mice, males were habituated to a testing environment for two hours then presented with one foreign C57BL6/J pup in the far corner of their homecage. When the male attacked the pup, the pup was removed from the cage and euthanized. Males were perfused 80-90 minutes after pup exposure and brains were postfixed overnight, cryoprotected in 30% sucrose overnight, and 60 µM sections were prepared on a sliding microtome. Tissue was stained with C-Fos antibody (see details in immunostaining section), imaged at 10X (Axioscan, Zeiss), and the number of C-Fos positive cells labeled with CTB-488 was quantified.

Monosynaptic input tracing

A 1:1 ratio (180 nL to cover the entire region) of AAV2.1-FLEx-TVA-mCherry (avian TVA receptor) and AAV2.1-FLEx-RG (rabies glycoprotein) was stereotaxically injected unilaterally into the PeFA

(Bregma coordinates AP: -0.6mm; ML: 0.3mm; DV: -4.2mm) of adult Ucn3::cre male and female mice (n=3/sex). Two weeks later, g-deleted rabies virus (deltaG-RV-eGFP) (300 nL) was injected into the same coordinate. Seven days later, mice were transcardially perfused with 4% paraformaldehyde. Tissue was post-fixed in PFA overnight and cryoprotected (30% sucrose) then serial sections were prepared on a freezing microtome (60 µm). Every third section (covering from the prefrontal cortex through the cerebellum) was imaged at 10X using the AxioScan (Zeiss). Cell bodies labeled by eGFP in anatomical areas were quantified and an input ratio was prepared by dividing the number of input cells in each region by the total number of input cells in each brain. Input ratio was compared across brain regions by One-way ANOVA followed by Dunnett's test for multiple comparisons and sexual dimorphisms compared using a two-tailed t-test.

Immunohistochemistry

C-Fos antibody staining

To visualize C-Fos protein in combination with CTB, perfused tissue was sliced on a freezing microtome at 30 µM, and every 3rd section throughout the perifornical area was stained. Briefly, sections were rinsed in PBS with 0.1% Triton (PBST), then blocked in 2% normal horse serum and 3% fetal bovine serum diluted in PBST for 2 hours at room temperature. Primary antibody Rabbit anti-C-Fos (Synaptic Systems) was diluted 1:2000 in PBS and sections were incubated for 72 hours at 4°C. After rinsing with PBST, secondary Anti-Rabbit A568 (1:1000) was applied at 1:1000 dilution in PBS for 48 hours at 4° C. Sections were rinsed in PBS, mounted to superfrost plus slides, coverslipped with Vectashield containing DAPI, and imaged (see details above).

GFP antibody staining

To amplify synaptophysin densities in the anterograde tracing experiments, the GFP signal was enhanced by antibody staining. Perfused tissue was sliced on a freezing microtome at 60 µM, and every 3rd section throughout the brain was stained. Briefly, sections were rinsed in PBS with 0.1% Triton (PBST), then blocked in 1.5% normal horse serum diluted in PBST for 1 hour (blocking solution) at room temperature. Primary antibody Rabbit anti-GFP (Novus Biologicals

NB600-308) was diluted 1:2000 in blocking solution and sections were incubated overnight at 4° C. After rinsing with PBST, secondary anti-Rabbit-A488 was applied at 1:200 dilution in blocking buffer and incubated overnight at 4° C. Sections were rinsed in PBS, mounted to superfrost plus slides, coverslipped with Vectashield containing DAPI, and imaged (see details above).

Oxytocin/vasopressin staining

Perfused tissue was sliced on a sliding microtome at 60 μM. Every 3rd section from the perifornical area was stained. Briefly, sections were rinsed in PBS with 0.1% Triton (PBST), then blocked in 10% fetal bovine serum diluted in PBST. Primary antibody Rabbit anti-vasopressin (Immunostar) or Rabbit anti-oxytocin (Millipore) were diluted 1:1000 in PBST and sections were incubated overnight at 4° C. After rinsing with PBST, secondary anti-Rabbit A647 was applied at 1:200 dilution in blocking buffer and incubated overnight at 4° C. Sections were rinsed in PBS, mounted to superfrost plus slides, coverslipped with Vectashield containing DAPI, and imaged on the Axioscan (Zeiss) at 10X magnification.

Electrophysiology

Solutions. We used modified ACSF (artificial cerebro-spinal fluid) contained (in mM): 105 choline chloride, 20 glucose, 24 $NaHCO_3$, 2.5 KCl, 0.5 $CaCl_2$, 8 $MgSO_4$, 5 sodium ascorbate, 3 sodium pyruvate, 1.25 NaH_2PO_4 (osmolarity 290, pH 7.35) for dissecting out the brain. All recordings were made in an oxygenated ACSF with composition (in mM): 115 NaCl, 2.5 KCl, 25 $NaHCO_3$, 1.25 NaH_2PO_4, 1 $MgSO_4$, 20 glucose, 2.0 $CaCl_2$ (osmolarity 290, pH 7.35).

Voltage clamp internal solution contained (in mM): 130 d-gluconic acid, 130 cesium hydroxide, 5.0 NaCl, 10 HEPES, 12 di-tris-phosphocreatine, 1 EGTA, 3.0 Mg-ATP, and 0.2 Na_3-GTP (osmolarity 291, pH 7.35). All chemicals were purchased from Sigma-Aldrich.

Acute brain slices. 8-12 weeks old Ucn3::Cre male (n =5) and female (n=3) mice were stereotaxically injected with AAV1-eF1a-DoubleFlox hChR2(H134R)-mCherry-WPRE-HgHpA (Addgene, Cambridge, MA) bilaterally into the PeFA (AP -0.6, ML ±0.3, DV -4.2; 200 nL). Mice recovered from surgery for 2-3 weeks and then sacrificed. Coronal brain slices were prepared using methods described previously (Kapoor and Urban, 2006). Mice were lightly anesthetized with isoflurane exposure using a vaporizer (Datex-Ohmeda) connected to a clear acrylic chamber for two min, and then deeply anesthetized with an i.p. injection of a mixture of ketamine (100 mg/kg) and xylazine (10 mg/kg). Ice-cold modified ACSF cutting solution was used to transcardially perfuse the mice, and brains were dissected into the same solution. Coronal slices (300 µm thick) were obtained using a vibratome (VT1000S; Leica, Germany) and collected in ice-cold cutting solution. After cutting, slices were incubated in oxygenated ACSF solution at 35 °C for 45 min and then at room temperature for the duration of the experiment.

***In vitro* recordings**. Whole-cell voltage-clamp recordings were made using borosilicate glass patch pipettes (6-10 Mohm) filled with internal solutions, respectively, and slices maintained at 35 °C in oxygenated ACSF. Slices were visualized under custom-built infrared optics on a BX51WI microscope (Olympus Optical, Tokyo, Japan). Recordings were obtained with a Multiclamp 700B amplifier (Molecular Devices, Palo Alto, CA), and physiological data were collected via software written in LabView (National Instruments) and pClamp 10.3 (Molecular Devices).

For optogenetic photostimulation experiments, ChR2 was activated using custom-built 465 nm (1-5mW/mm^2, CBT-90-B-L11, Luminus) light source. Light pulses of 5-20ms, delivered at 2-20 Hz, were used to probe synaptic connectivity. We used Wilcoxon rank-sum test to compare the distributions.

For chemogenetics stimulation experiments, 8-12 weeks old Ucn3::Cre male mice were stereotaxically injected with pAAV-hSyn-DIO-hM3D(Gq)-mCherry (Addgene, Cambridge, MA)

bilaterally into the PeFA (AP -0.6, ML ±0.3, DV -4.2; 200 nL). For the stock solutions, CNO (clozapine-*n*-oxide) was dissolved at 0.5 mg/ml concentrations in ACSF and was further diluted to 10 μM in ACSF for the experiments. We measured the effects of CNO on Ucn3::Cre * hChR2(H134R)-mCherry neurons by selectively recording from mCherry positive neruons in PeFA. The recording protocol included, 3-5 minutes of baseline followed by 3-5 minutes of bath application of 10 μM CNO and 3-5 minutes of washout of CNO. We used Wilcoxon rank-sum test to compare the distributions of firing rate.

Statistics

In our molecular studies, we used One-way ANOVA followed by Tukey post-hoc test or Kruskal-Wallis test followed by Dunn's post-hoc test. Details for differential gene expression for the microarray analysis are explained under "Microarray" in the methods section. Similarly, the pS6 data analysis is described in the "pS6 pulldowns and RNASeq analysis" section.

For most optogenetics behavior studies, we used repeated One- or Two-Way ANOVA analyses followed by Bonferroni or Tukey post-hoc tests. For the pup retrieval percentage data, we used a Friedman test. To compare numbers of animals retrieving across 2 trials, we used a Fisher's exact test or Chi-Square test, and across 3 trials, we used an accelerated failure regression model. For DREADD experiments, we used t-test or Mann-Whitney test.

For the projection and input data, we used regression analysis.

For electrophysiology analysis, we used 2- sided Wilcoxon rank sum test to compare the amplitudes of evoked EPSCs across regions (LS, VMH and Ahi) and for comparing the amplitudes of EPSCs in paired pulse paradigm.

Replication and outliers

For molecular experiments, we used 3-6 biological replicates (mice) per group. For animal behavior experiments, we used 9-12 animals per group based on our previous experience with studying parental behavior. For all experiments, both molecular and behavioral, experiments were performed in at least two cohorts if not more.

For molecular experiments, outliers were determined using a Grubb's outlier test. For behavioral experiments, mice were excluded if post-hoc analysis revealed insufficient viral infection.

Abbreviations in the text

Brain region abbreviations: MPOA, medial preoptic area; VLPO, ventrolateral preoptic area; Pe, periventricular nucleus; LSv, ventral lateral septum; LSi, intermediate lateral septum; BNSTm, medial bed nucleus stria terminalis; PeFA, perifornical area; PVH, paraventricular hypothalamus; DMH, dorsomedial hypothalamus; VMH, ventromedial hypothalamus; AH, anterior hypothalamus; LH, lateral hypothalamus; PLH, peduncular lateral hypothalamus; ZI, zona incerta; MeAPD, posterodorsal medial amygdala; MeAPV, posteroventral medial amygdala; Arc, arcuate nucleus; PMv, ventral premammillary nucleus; ME, median eminence; PH, posterior hypothalamus; AHi, amygdalohippocampal area.

Frequently mentioned genes: Ucn3, Urocortin-3; Gal, Galanin; Oxt, Oxytocin; Avp, Vasopressin; Trh, Thyrotropin releasing hormone; Crh, Corticotropin releasing hormone.

Electrophysiology: sEPSC, spontaneous excitatory post synaptic current and eEPSC, evoked post synaptic current.

REFERENCES

Albert, D.J. & Chew, G.L. (1980) The septal forebrain and the inhibitory modulation of attack and defense in the rat. A review. *Behav Neural Biol*, **30**, 357-388.

Amano, T., Shindo, S., Yoshihara, C., Tsuneoka, Y., Uki, H., Minami, M. & Kuroda, K.O. (2017) Development-dependent behavioral change toward pups and synaptic transmission in the rhomboid nucleus of the bed nucleus of the stria terminalis. *Behav Brain Res*, **325**, 131-137.

Anthony, T.E., Dee, N., Bernard, A., Lerchner, W., Heintz, N. & Anderson, D.J. (2014) Control of stress-induced persistent anxiety by an extra-amygdala septohypothalamic circuit. *Cell*, **156**, 522-536.

Battagello, D.S., Diniz, G.B., Candido, P.L., da Silva, J.M., de Oliveira, A.R., Torres da Silva, K.R., Lotfi, C.F.P., de Oliveira, J.A., Sita, L.V., Casatti, C.A., Lovejoy, D.A. & Bittencourt, J.C. (2017) Anatomical Organization of Urocortin 3-Synthesizing Neurons and Immunoreactive Terminals in the Central Nervous System of Non-Human Primates [Sapajus spp.]. *Front Neuroanat*, **11**, 57.

Betley, J.N., Cao, Z.F., Ritola, K.D. & Sternson, S.M. (2013) Parallel, redundant circuit organization for homeostatic control of feeding behavior. *Cell*, **155**, 1337-1350.

Blanchard, D.C., Blanchard, R.J., Takahashi, L.K. & Takahashi, T. (1977) Septal lesions and aggressive behavior. *Behav Biol*, **21**, 157-161.

Bloch, M., Daly, R.C. & Rubinow, D.R. (2003) Endocrine factors in the etiology of postpartum depression. *Compr Psychiatry*, **44**, 234-246.

Canteras, N.S., Chiavegatto, S., Ribeiro do Valle, L.E. & Swanson, L.W. (1997) Severe reduction of rat defensive behavior to a predator by discrete hypothalamic chemical lesions. *Brain Res Bull*, **44**, 297-305.

Carvalho, B.S. & Irizarry, R.A. (2010) A framework for oligonucleotide microarray preprocessing. *Bioinformatics*, **26**, 2363-2367.

Chen, P., Lin, D., Giesler, J. & Li, C. (2011) Identification of urocortin 3 afferent projection to the ventromedial nucleus of the hypothalamus in rat brain. *J Comp Neurol*, **519**, 2023-2042.

Chen, P.B., Hu, R.K., Wu, Y.E., Pan, L., Huang, S., Micevych, P.E. & Hong, W. (2019) Sexually Dimorphic Control of Parenting Behavior by the Medial Amygdala. *Cell*, **176**, 1206-1221 e1218.

Deussing, J.M., Breu, J., Kuhne, C., Kallnik, M., Bunck, M., Glasl, L., Yen, Y.C., Schmidt, M.V., Zurmuhlen, R., Vogl, A.M., Gailus-Durner, V., Fuchs, H., Holter, S.M., Wotjak, C.T., Landgraf, R., de Angelis, M.H., Holsboer, F. & Wurst, W. (2010) Urocortin 3 modulates social discrimination abilities via corticotropin-releasing hormone receptor type 2. *The Journal of neuroscience : the official journal of the Society for Neuroscience*, **30**, 9103-9116.

Dobin, A., Davis, C.A., Schlesinger, F., Drenkow, J., Zaleski, C., Jha, S., Batut, P., Chaisson, M. & Gingeras, T.R. (2013) STAR: ultrafast universal RNA-seq aligner. *Bioinformatics*, **29**, 15-21.

Donaldson, Z.R. & Young, L.J. (2008) Oxytocin, vasopressin, and the neurogenetics of sociality. *Science*, **322**, 900-904.

Dulac, C., O'Connell, L.A. & Wu, Z. (2014) Neural control of maternal and paternal behaviors. *Science*, **345**, 765-770.

Elwood, R.W. (1994) Temporal-based kinship recognition: A switch in time saves mine. *Behav Processes*, **33**, 15-24.

Fang, Y.Y., Yamaguchi, T., Song, S.C., Tritsch, N.X. & Lin, D. (2018) A Hypothalamic Midbrain Pathway Essential for Driving Maternal Behaviors. *Neuron*, **98**, 192-207 e110.

Fekete, E.M., Inoue, K., Zhao, Y., Rivier, J.E., Vale, W.W., Szucs, A., Koob, G.F. & Zorrilla, E.P. (2007) Delayed satiety-like actions and altered feeding microstructure by a selective type 2 corticotropin-releasing factor agonist in rats: intra-hypothalamic urocortin 3 administration reduces food intake by prolonging the post-meal interval. *Neuropsychopharmacology*, **32**, 1052-1068.

Fleming, A.S. & Rosenblatt, J.S. (1974a) Olfactory regulation of maternal behavior in rats. I. Effects of olfactory bulb removal in experienced and inexperienced lactating and cycling females. *Journal of comparative and physiological psychology*, **86**, 221-232.

Fleming, A.S. & Rosenblatt, J.S. (1974b) Olfactory regulation of maternal behavior in rats. II. Effects of peripherally induced anosmia and lesions of the lateral olfactory tract in pup-induced virgins. *Journal of comparative and physiological psychology*, **86**, 233-246.

Fleming, A.S., Vaccarino, F. & Luebke, C. (1980) Amygdaloid inhibition of maternal behavior in the nulliparous female rat. *Physiology & behavior*, **25**, 731-743.

Gammie, S.C. & Nelson, R.J. (2001) cFOS and pCREB activation and maternal aggression in mice. *Brain research*, **898**, 232-241.

Heasley, J.E. (1983) Energy Allocation in Response to Reduced Food Intake in Pregnant and Lactating Laboratory Mice. *Acta Theriologica*, **28**, 55-71.

Horii-Hayashi, N., Nomoto, K., Endo, N., Yamanaka, A., Kikusui, T. & Nishi, M. (2021) Hypothalamic perifornical Urocortin-3 neurons modulate defensive responses to a potential threat stimulus. *iScience*, **24**, 101908.

Hrdy, S.B. (1974) Male-male competition and infanticide among the langurs (Presbytis entellus) of Abu, Rajasthan. *Folia Primatol (Basel)*, **22**, 19-58.

Hrdy, S.B. (1979) Infanticide among animals: A review, classification, and examination of the implications for the reproductive strategy of females. *Ethology and Sociobiology*, **1**, 13-40.

Hutchens, B.F. & Kearney, J. (2020) Risk Factors for Postpartum Depression: An Umbrella Review. *J Midwifery Womens Health*, **65**, 96-108.

Insel, T.R. (2010) The challenge of translation in social neuroscience: a review of oxytocin, vasopressin, and affiliative behavior. *Neuron*, **65**, 768-779.

Irizarry, R.A., Hobbs, B., Collin, F., Beazer-Barclay, Y.D., Antonellis, K.J., Scherf, U. & Speed, T.P. (2003) Exploration, normalization, and summaries of high density oligonucleotide array probe level data. *Biostatistics*, **4**, 249-264.

Isogai, Y., Si, S., Pont-Lezica, L., Tan, T., Kapoor, V., Murthy, V.N. & Dulac, C. (2011) Molecular organization of vomeronasal chemoreception. *Nature*, **478**, 241-245.

Isogai, Y., Wu, Z., Love, M.I., Ahn, M.H., Bambah-Mukku, D., Hua, V., Farrell, K. & Dulac, C. (2018) Multisensory Logic of Infant-Directed Aggression by Males. *Cell*, **175**, 1827-1841 e1817.

Jamieson, P.M., Cleasby, M.E., Kuperman, Y., Morton, N.M., Kelly, P.A., Brownstein, D.G., Mustard, K.J., Vaughan, J.M., Carter, R.N., Hahn, C.N., Hardie, D.G., Seckl, J.R., Chen, A. & Vale, W.W. (2011) Urocortin 3 transgenic mice exhibit a metabolically favourable phenotype resisting obesity and hyperglycaemia on a high-fat diet. *Diabetologia*, **54**, 2392-2403.

Jezova, D., Skultetyova, I., Tokarev, D.I., Bakos, P. & Vigas, M. (1995) Vasopressin and oxytocin in stress. *Ann N Y Acad Sci*, **771**, 192-203.

Knight, Z.A., Tan, K., Birsoy, K., Schmidt, S., Garrison, J.L., Wysocki, R.W., Emiliano, A., Ekstrand, M.I. & Friedman, J.M. (2012) Molecular profiling of activated neurons by phosphorylated ribosome capture. *Cell*, **151**, 1126-1137.

Kohl, J., Autry, A.E. & Dulac, C. (2017) The neurobiology of parenting: A neural circuit perspective. *Bioessays*, **39**, 1-11.

Kohl, J., Babayan, B.M., Rubinstein, N.D., Autry, A.E., Marin-Rodriguez, B., Kapoor, V., Miyamishi, K., Zweifel, L.S., Luo, L., Uchida, N. & Dulac, C. (2018) Functional circuit architecture underlying parental behaviour. *Nature*, **556**, 326-331.

König, B. (1989) Behavioural ecology of kin recognition in house mice. *Ethology Ecology & Evolution*, **1**, 99-110.

Kruk, M.R., Van der Poel, A.M., Meelis, W., Hermans, J., Mostert, P.G., Mos, J. & Lohman, A.H. (1983) Discriminant analysis of the localization of aggression-inducing electrode placements in the hypothalamus of male rats. *Brain research*, **260**, 61-79.

Kuperman, Y., Issler, O., Regev, L., Musseri, I., Navon, I., Neufeld-Cohen, A., Gil, S. & Chen, A. (2010) Perifornical Urocortin-3 mediates the link between stress-induced anxiety and energy homeostasis. *Proc Natl Acad Sci U S A*, **107**, 8393-8398.

Lee, H., Kim, D.W., Remedios, R., Anthony, T.E., Chang, A., Madisen, L., Zeng, H. & Anderson, D.J. (2014) Scalable control of mounting and attack by Esr1+ neurons in the ventromedial hypothalamus. *Nature*, **509**, 627-632.

Lin, D., Boyle, M.P., Dollar, P., Lee, H., Lein, E.S., Perona, P. & Anderson, D.J. (2011) Functional identification of an aggression locus in the mouse hypothalamus. *Nature*, **470**, 221-226.

Lonstein, J.S. & De Vries, G.J. (2000) Sex differences in the parental behavior of rodents. *Neurosci Biobehav Rev*, **24**, 669-686.

Lukas, D. & Huchard, E. (2018) The evolution of infanticide by females in mammals. *bioRxiv*, 405688.

Marlin, B.J., Mitre, M., D'Amour J, A., Chao, M.V. & Froemke, R.C. (2015) Oxytocin enables maternal behaviour by balancing cortical inhibition. *Nature*, **520**, 499-504.

Marsteller, F.A. & Lynch, C.B. (1987) Reproductive responses to variation in temperature and food supply by house mice: II. Lactation. *Biol Reprod*, **37**, 844-850.

Mudge, J.M. & Harrow, J. (2015) Creating reference gene annotation for the mouse C57BL6/J genome assembly. *Mamm Genome*, **26**, 366-378.

Noirot, E. (1972) The Onset of Maternal Behavior in Rats, Hamsters, and Mice A Selective Review. *Advances in the Study of Behavior*, **4**, 107-145.

Numan, M. (2020) *The parental brain : mechanisms, development, and evolution*. Oxford University Press, New York.

Okabe, S., Kitano, K., Nagasawa, M., Mogi, K. & Kikusui, T. (2013) Testosterone inhibits facilitating effects of parenting experience on parental behavior and the oxytocin neural system in mice. *Physiology & behavior*, **118**, 159-164.

Parmigiani, S. & Vom Saal, F.S. (1994) *Infanticide and parental care*. Harwood Academic Publishers, Chur, Switzerland ; Langhorne, Pa., USA.

Perez, J.D., Rubinstein, N.D., Fernandez, D.E., Santoro, S.W., Needleman, L.A., Ho-Shing, O., Choi, J.J., Zirlinger, M., Chen, S.K., Liu, J.S. & Dulac, C. (2015) Quantitative and functional interrogation of parent-of-origin allelic expression biases in the brain. *Elife*, **4**, e07860.

Phipson, B., Lee, S., Majewski, I.J., Alexander, W.S. & Smyth, G.K. (2016) Robust Hyperparameter Estimation Protects against Hypervariable Genes and Improves Power to Detect Differential Expression. *Ann Appl Stat*, **10**, 946-963.

Ritchie, M.E., Phipson, B., Wu, D., Hu, Y., Law, C.W., Shi, W. & Smyth, G.K. (2015) limma powers differential expression analyses for RNA-sequencing and microarray studies. *Nucleic Acids Res*, **43**, e47.

Sato, K., Hamasaki, Y., Fukui, K., Ito, K., Miyamichi, K., Minami, M. & Amano, T. (2020) Amygdalohippocampal Area Neurons That Project to the Preoptic Area Mediate Infant-Directed Attack in Male Mice. *J Neurosci*, **40**, 3981-3994.

Scarff, J.R. (2019) Postpartum Depression in Men. *Innov Clin Neurosci*, **16**, 11-14.

Scott, N., Prigge, M., Yizhar, O. & Kimchi, T. (2015) A sexually dimorphic hypothalamic circuit controls maternal care and oxytocin secretion. *Nature*, **525**, 519-522.

Slotnick, B.M., McMullen, M.F. & Fleischer, S. (1973) Changes in emotionality following destruction of the septal area in albino mice. *Brain Behav Evol*, **8**, 241-252.

Stagkourakis, S., Smiley, K.O., Williams, P., Kakadellis, S., Ziegler, K., Bakker, J., Brown, R.S.E., Harkany, T., Grattan, D.R. & Broberger, C. (2020) A Neuro-hormonal Circuit for Paternal Behavior Controlled by a Hypothalamic Network Oscillation. *Cell*, **182**, 960-975 e915.

Svare, B., Bartke, A. (1978) Food deprivation induces conspecific killing in mice. *Aggressive Behavior*, **4**, 253-261.

Swanson, L.W. & Sawchenko, P.E. (1980) Paraventricular nucleus: a site for the integration of neuroendocrine and autonomic mechanisms. *Neuroendocrinology*, **31**, 410-417.

Tachikawa, K.S., Yoshihara, Y. & Kuroda, K.O. (2013) Behavioral transition from attack to parenting in male mice: a crucial role of the vomeronasal system. *The Journal of neuroscience : the official journal of the Society for Neuroscience*, **33**, 5120-5126.

Tsuneoka, Y., Tokita, K., Yoshihara, C., Amano, T., Esposito, G., Huang, A.J., Yu, L.M., Odaka, Y., Shinozuka, K., McHugh, T.J. & Kuroda, K.O. (2015) Distinct preoptic-BST nuclei dissociate paternal and infanticidal behavior in mice. *EMBO J*, **34**, 2652-2670.

Turro, E., Astle, W.J. & Tavare, S. (2014) Flexible analysis of RNA-seq data using mixed effects models. *Bioinformatics*, **30**, 180-188.

Turro, E., Su, S.Y., Goncalves, A., Coin, L.J., Richardson, S. & Lewin, A. (2011) Haplotype and isoform specific expression estimation using multi-mapping RNA-seq reads. *Genome Biol*, **12**, R13.

Ulrich-Lai, Y.M. & Herman, J.P. (2009) Neural regulation of endocrine and autonomic stress responses. *Nat Rev Neurosci*, **10**, 397-409.

Vale, W., Spiess, J., Rivier, C. & Rivier, J. (1981) Characterization of a 41-residue ovine hypothalamic peptide that stimulates secretion of corticotropin and beta-endorphin. *Science*, **213**, 1394-1397.

Venihaki, M., Sakihara, S., Subramanian, S., Dikkes, P., Weninger, S.C., Liapakis, G., Graf, T. & Majzoub, J.A. (2004) Urocortin III, a brain neuropeptide of the corticotropin-releasing hormone family: modulation by stress and attenuation of some anxiety-like behaviours. *J Neuroendocrinol*, **16**, 411-422.

vom Saal, F.S. (1985) Time-contingent change in infanticide and parental behavior induced by ejaculation in male mice. *Physiology & behavior*, **34**, 7-15.

Wagner, G.P., Kin, K. & Lynch, V.J. (2012) Measurement of mRNA abundance using RNA-seq data: RPKM measure is inconsistent among samples. *Theory Biosci*, **131**, 281-285.

Wang, L., Chen, I.Z. & Lin, D. (2015) Collateral pathways from the ventromedial hypothalamus mediate defensive behaviors. *Neuron*, **85**, 1344-1358.

Wickersham, I.R., Lyon, D.C., Barnard, R.J., Mori, T., Finke, S., Conzelmann, K.K., Young, J.A. & Callaway, E.M. (2007) Monosynaptic restriction of transsynaptic tracing from single, genetically targeted neurons. *Neuron*, **53**, 639-647.

Wittmann, G., Fuzesi, T., Liposits, Z., Lechan, R.M. & Fekete, C. (2009) Distribution and axonal projections of neurons coexpressing thyrotropin-releasing hormone and urocortin 3 in the rat brain. *J Comp Neurol*, **517**, 825-840.

Wu, Z., Autry, A.E., Bergan, J.F., Watabe-Uchida, M. & Dulac, C.G. (2014) Galanin neurons in the medial preoptic area govern parental behaviour. *Nature*, **509**, 325-330.

Yang, C.F., Chiang, M.C., Gray, D.C., Prabhakaran, M., Alvarado, M., Juntti, S.A., Unger, E.K., Wells, J.A. & Shah, N.M. (2013) Sexually dimorphic neurons in the ventromedial hypothalamus govern mating in both sexes and aggression in males. *Cell*, **153**, 896-909.

Yoshihara, C., Tokita, K., Maruyama, T., Kaneko, M., Tsuneoka, Y., Fukumitsu, K., Miyazawa, E., Shinozuka, K., Huang, A.J., Nishimori, K., McHugh, T.J., Tanaka, M., Itohara, S., Touhara, K., Miyamichi, K. & Kuroda, K.O. (2021) Calcitonin receptor signaling in the medial preoptic area enables risk-taking maternal care. *Cell Rep*, **35**, 109204.

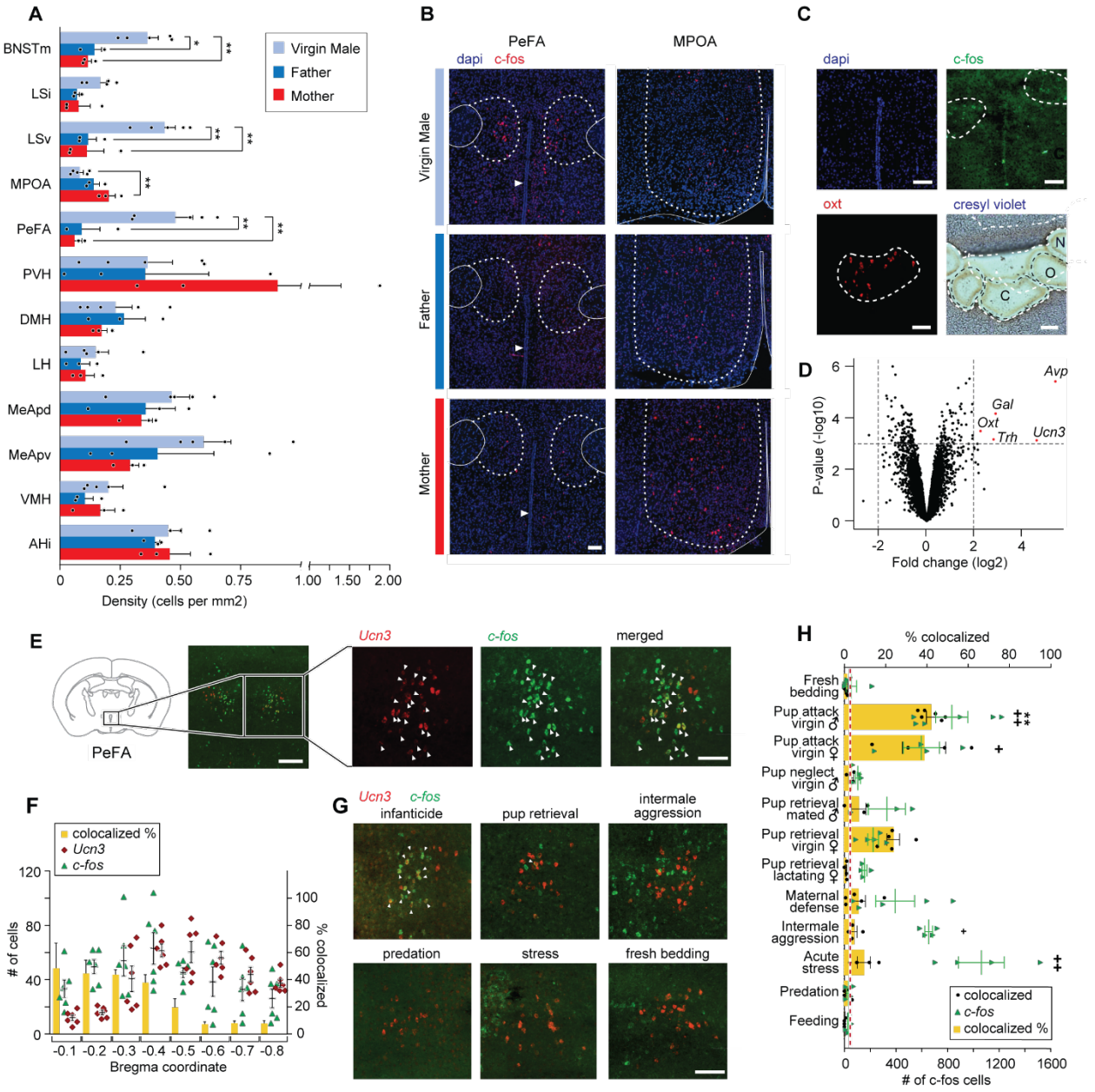

Figure 1. The neuropeptide gene *urocortin-3* (*Ucn3*) in the perifornical area (PeFA) marks neurons activated during infanticide.

A. Quantification of *c-fos*+ cells per mm^2 in brain areas of interest (oriented from top to bottom, rostral to caudal) in virgin males (attacking), mated males (parental), and mated females (parental) after pup exposure. One-way ANOVA followed by Tukey's multiple comparison test reveals significant differences in the number of *c-fos*+ cells identified between parental and infanticidal animals in medial bed nucleus of

stria terminalis (BNSTm) ($F_{2,8}$=12.47, p<0.0035), ventral lateral septum (LSv) ($F_{2,8}$=14.31, p<0.0023), medial preoptic area (MPOA) ($F_{2,8}$=8.536, p<0.0104), and perifornical area (PeFA) ($F_{2,8}$=12.02, p<0.0039) (virgin male n=5; fathers n=3; mothers n=3). B. Representative in situ hybridization images of *c-fos* (red channel) expression in PeFA and MPOA after animal exposure to pups with counterstain DAPI (blue channel) (scale bar: 100μm). Dotted lines in right and left denote the boundary of brain regions of interest (PeFA and MPOA respectively), solid lines denote the fornix, arrowheads indicate location of third ventricle in the left panels, and solid lines denote the edge of the brain and third ventricle in the right panel. C. Laser capture microscopy strategy to identify markers of cells activated during infanticide (scale bar 100μm). Tissue material corresponding to areas labelled by *c-fos* (C) after pup-mediated attack, as well as oxytocin+ (Oxt) (O) and adjacent negative (N) area was laser-dissected and the corresponding transcripts characterized by microarray analysis. D. Volcano plot showing the fold change (log base 2) against the p-value (log base 10) for all genes. Transcripts with greater than a 2-fold change in expression in the *c-fos*+ compared to negative region and a p-value smaller than 0.001 are shown in red: *vasopressin* (*Avp*), *thyrotropin-releasing hormone* (*Trh*), *galanin* (*Gal*), *Oxt* and *Ucn3* (n=3 biological replicates, each containing pooled tissue from 6 males). E. Representative *in situ* hybridization showing colocalization of *Ucn3* (red) and *c-fos* (green) expression after infanticide (scale bar 100 μm), arrowheads indicate colocalization. F. Plot depicting number (#) of neurons expressing *c-fos* (green triangles), *Ucn3* (red circles) and percent (%) of cells expressing both *c-fos* and *Ucn3* (yellow bars) per brain section across bregma coordinates (n=6) indicates high colocalization in rostral PeFA. Overall representation of *Ucn3*+ neurons in the PeFA (2.74%) is indicated by red line). G. Representative in situ hybridization showing expression of *Ucn3* (red) and *c-fos* (green) after infanticide and other behaviors in the rostral PeFA, with colocalization (white arrowheads) only observed after infanticide (scale bar 100 μm). H. Percentage of *Ucn3*+ cells colocalized with *c-fos* after various behaviors (yellow bars; significance *) and number of *c-fos* cells induced by various behaviors across sections of the rostral PeFA (green triangles; significance #) (n=3-6/group). Kruskal-Wallis test followed by Dunn's multiple comparisons test reveals significant differences in number of *c-fos*+ cells in rostral PeFA between fresh bedding control exposure and pup attack in virgin males and virgin females, intermale aggression and acute stress (p<0.0001; #);

yet, despite the observed widespread activation of PeFA cells during various behaviors, only pup-directed attacks by virgin males induced significant *c-fos* expression in PeFA^{Ucn3} neurons ($p<0.0002$; *).

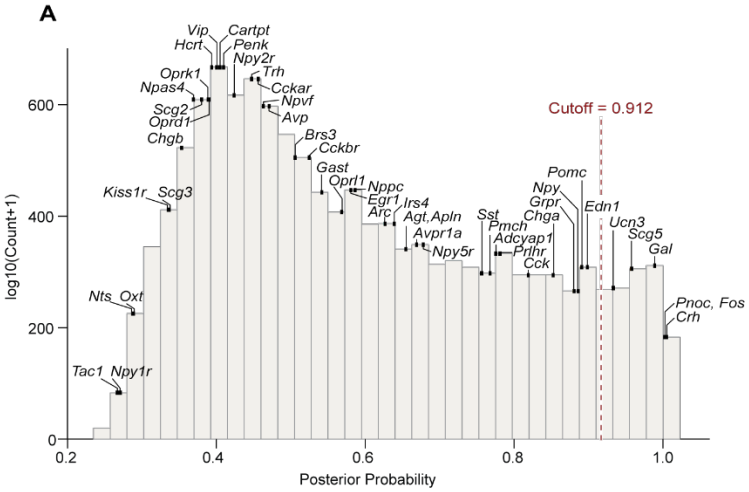

B

Marker$^+$	% of *c-fos*$^+$ cells expressing marker	% of marker$^+$ cells expressing *c-fos*
Ucn3	55.3	52.5
Trh	53.3	45.5
Gal	20.8	42.8
Pdyn	17.9	27.7
Cart	5.0	11.5
Crf	3.3	10.5
Sst	2.7	4.1
Oxt	1.6	1.8
Penk	0.8	5.3
Avp	7.5	5.1

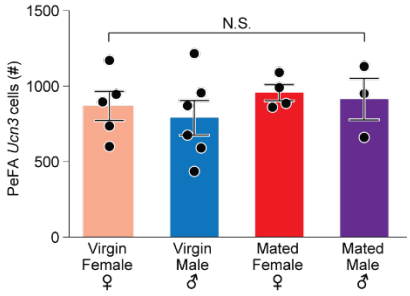

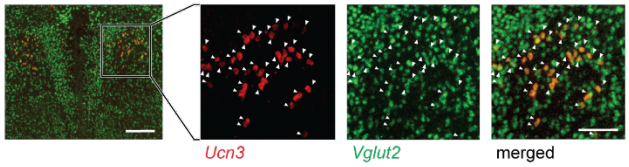

E

	Coloc %	*Ucn3* %	p-value
Fresh bedding	1.23	2.74	<0.0001
Pup attack virgin male	42.03	2.74	<0.0001
Pup attack virgin female	38.63	2.74	<0.0001
Pup neglect virgin male	3.21	2.74	<0.0001
Pup retrieval mated male	6.96	2.74	<0.0001
Pup retrieval virgin female	23.70	2.74	<0.0001
Pup retrieval lactating female	0.85	2.74	0.0785
Maternal defense	6.77	2.74	<0.0001
Intermale aggression	4.68	2.74	0.0036
Acute stress	9.43	2.74	<0.0001
Predation	1.47	2.74	<0.0001
Feeding	0.16	2.74	0.5339

Figure 1—figure supplement 1. A. Distribution of the posterior probabilities of expression levels expressed as log10(Counts) in immunoprecipitated (IP) minus input in infanticidal males exposed to pups

compared to males exposed to fresh bedding. Vertical, red-dashed line marks the empirically defined significant posterior-probability cutoff. Expression of neuropeptides and their receptors is indicated by their posterior probabilities. B. Relative enrichment in infanticide-induced *c-fos* and candidate marker gene expression in PeFA neurons. C. Analysis of the number of *Ucn3*+ neurons in the PeFA among virgin and mated males and females reveals no significant difference. D. Representative in situ hybridization images showing *Ucn3* (red) co-expression with *Vglut2* (green) in the PeFA (scale bar 100 µm), arrowheads indicate colocalization. E. Colocalization of *c-fos* and *Ucn3* expression (Coloc %) relative to the representation of *Ucn3*+ neurons in the total pool of PeFA neurons (*Ucn3*).

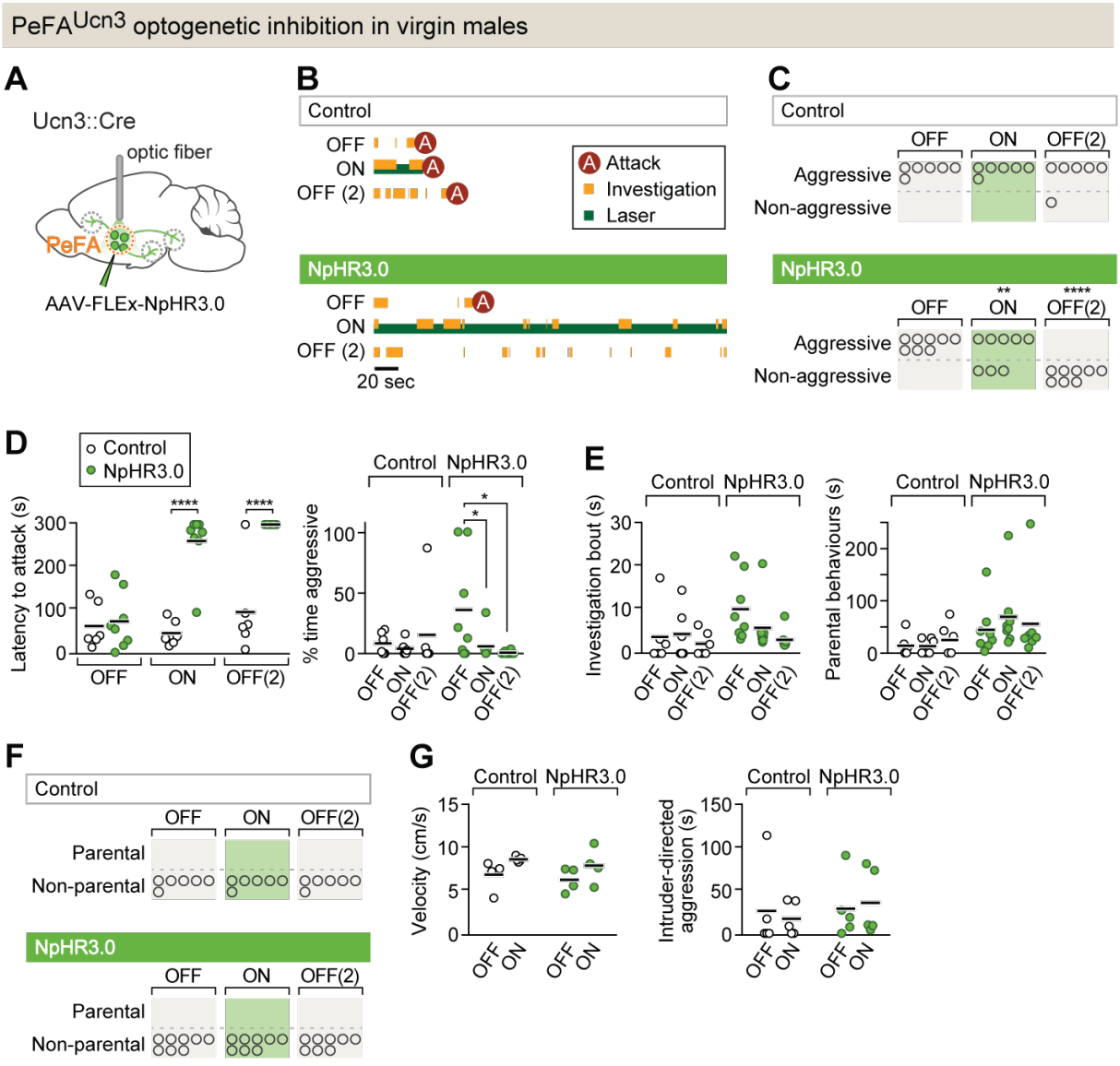

Figure 2. PeFA^{Ucn3} neurons are required for infant-directed aggression in virgin males.

A. Setup for optogenetic silencing of PeFA^{Ucn3} neurons in infanticidal virgin males. B. Representative behavior trace of a control and a NpHR3.0-expressing male across 3 consecutive sessions (scale bar 20 sec of 5 min test). C. Numbers of control and NpHR3.0-expressing males showing aggressive pup-directed behavior (accelerated failure regression model with first session as time-point baseline and controls as treatment baseline, significant difference between control (n=6) and NpHR3.0 (n=8) during laser inhibition

p<0.01 and during second laser off session p<0.0005). D. (left) Pup-directed attack latency across sessions comparing control (open dots) and NpHR3.0 (green dots) infected males. Two-way repeated measures ANOVA control vs. NpHR3.0 $F_{(1,12)}$=35.05, p<0.0001, sessions $F_{(2,24)}$=22.71, p<0.0001, and interaction $F_{(2,24)}$=17.30, p<0.0001 followed by Bonferroni's multiple comparisons test. (right) Percentage of time displaying aggression toward pups across 3 sessions in control (open dots) and NpHR3.0 (green dots) males. Two-way repeated measures ANOVA showed no main effect while post-hoc Tukey's multiple comparisons test revealed significant differences between sessions in the NpHR3.0 group. E. (left) Pup investigation bout length across 3 sessions in control and NpHR3.0 males. (right) Duration of parental care behaviors across 3 sessions in control and NpHR3.0 males. F. Number of males in control and NpHR3.0-expressing groups displaying parental behaviors. G. (left) Locomotion velocity in control and NpHR3.0-expressing males with and without laser stimulation. (right) Duration of aggressive displays during adult male interactions in control and NpHR3.0-expressing males with and without laser stimulation.

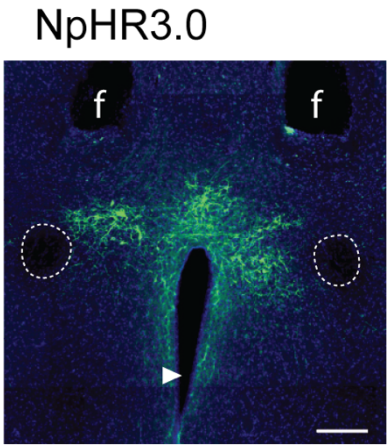

Figure 2—figure supplement 2.

Representative image of AAV-mediated NpHR3.0 expression in the PeFA of Ucn3::Cre males (scale bar 100 μm). Fornix indicated by outline, arrowhead indicates ventricle, f denotes fiber tract.

PeFA^{Ucn3} optogenetic activation in virgin females

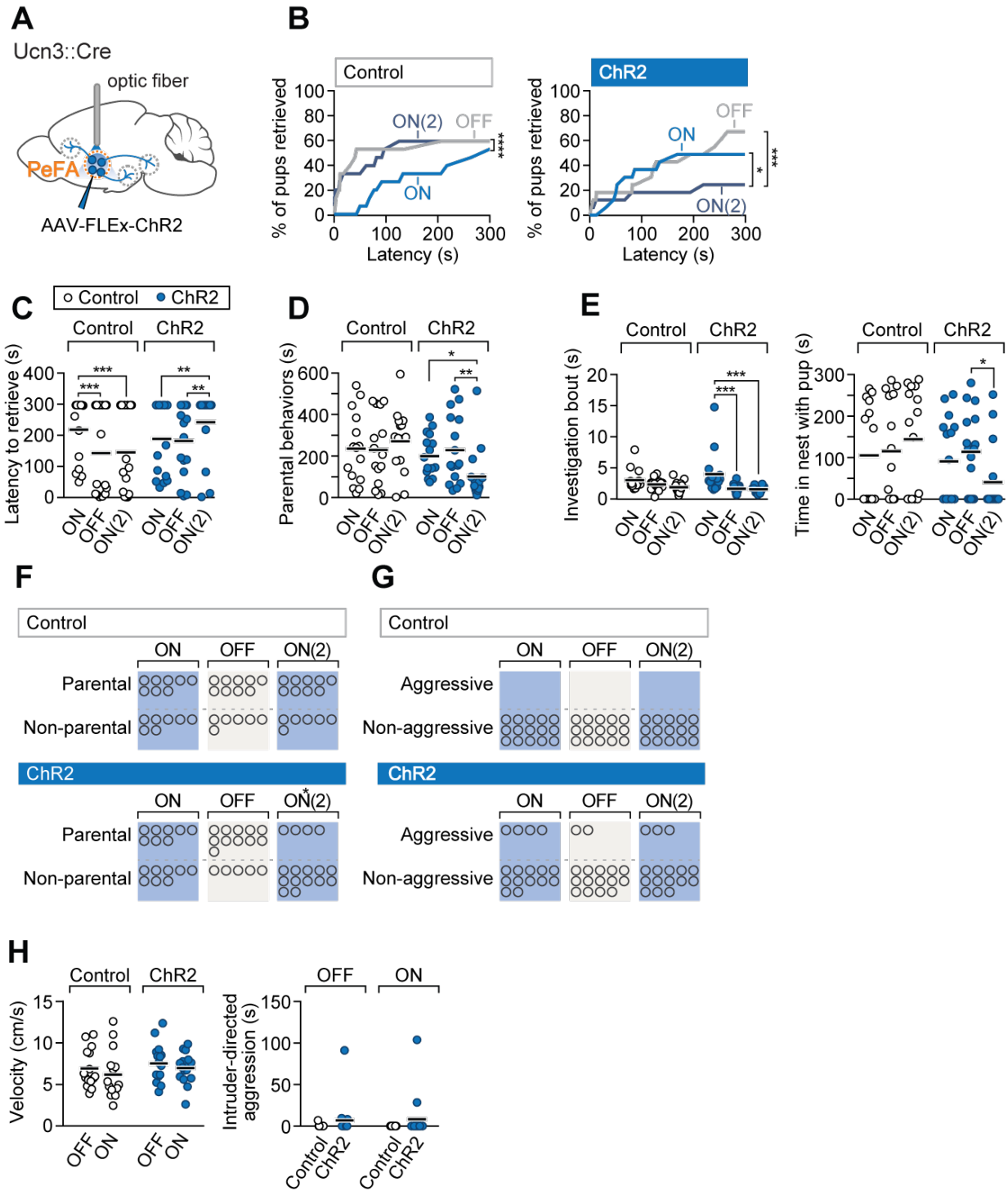

Figure 3. PeFA^{Ucn3} optogenetic activation in virgin females suppresses parental behavior.

A. Setup for optogenetic activation of PeFA^{Ucn3} neurons in virgin female mice. B. (Left) Cumulative retrieval of pups in virgin females injected with a control virus (n=15). Friedman statistic$_{(3, 27)}$ = 41.84 followed by Dunn's multiple comparisons tests. (right) Cumulative retrieval of pups in virgin females injected with conditional virus expressing ChR2 (n=16). Friedman statistic $_{(3, 24)}$ = 17.19, followed by Dunn's multiple comparisons test. C. Latency to retrieve in control (open dots) and ChR2-expressing (blue dots) females across three sessions. Two-way repeated measures ANOVA reveals no main effect of virus treatment F_{1-29}=0.7892, but significant effects of session $F_{2,58}$=6.181 (p=0.0037) and interaction $F_{2,58}$=13.42 (p<0.0001). Post-hoc analysis Bonferroni's multiple comparisons. D. Duration of parental behaviors displayed by control (open dots) and ChR2-expressing (blue dots) females. Two-way repeated measures ANOVA reveals no main effect of virus F1-29=2.721 or session $F_{2,58}$=1.178, but a significant main interaction effect $F^{2,58}$=4.747 (p=0.0123) followed by Tukey's post-hoc analysis. E. (left) Duration of time spent investigating pups in a single bout across three sessions in control (open dots) versus ChR2 (blue dots) females. Two-way repeated measures ANOVA reveals no significant main effect of virus treatment F_{1-29}=1.637 or session $F_{2,58}$=0.6324, but a significant interaction effect $F_{2,58}$=3.746 (p=0.0295). Post-hoc analysis Tukey's multiple comparisons test. (right) Time spent in the nest with pups. Two-way repeated measures ANOVA shows a significant main interaction effect $F_{2,58}$=3.746 (p<0.03). Post-hoc analysis by Tukey's multiple comparisons test. F. Number of females displaying parental behaviors across three sessions in control and ChR2 females (accelerated failure regression model with first session as time-point baseline and control as treatment baseline, significant difference between control and ChR2 females in second laser on session p<0.04). G. Number of females in control or ChR2 groups displaying aggressive behaviors toward pups. H. (left) Locomotion velocity in control or ChR2 females with or without laser stimulation is not significantly affected. (right) Aggression toward an adult male intruder is unaffected.

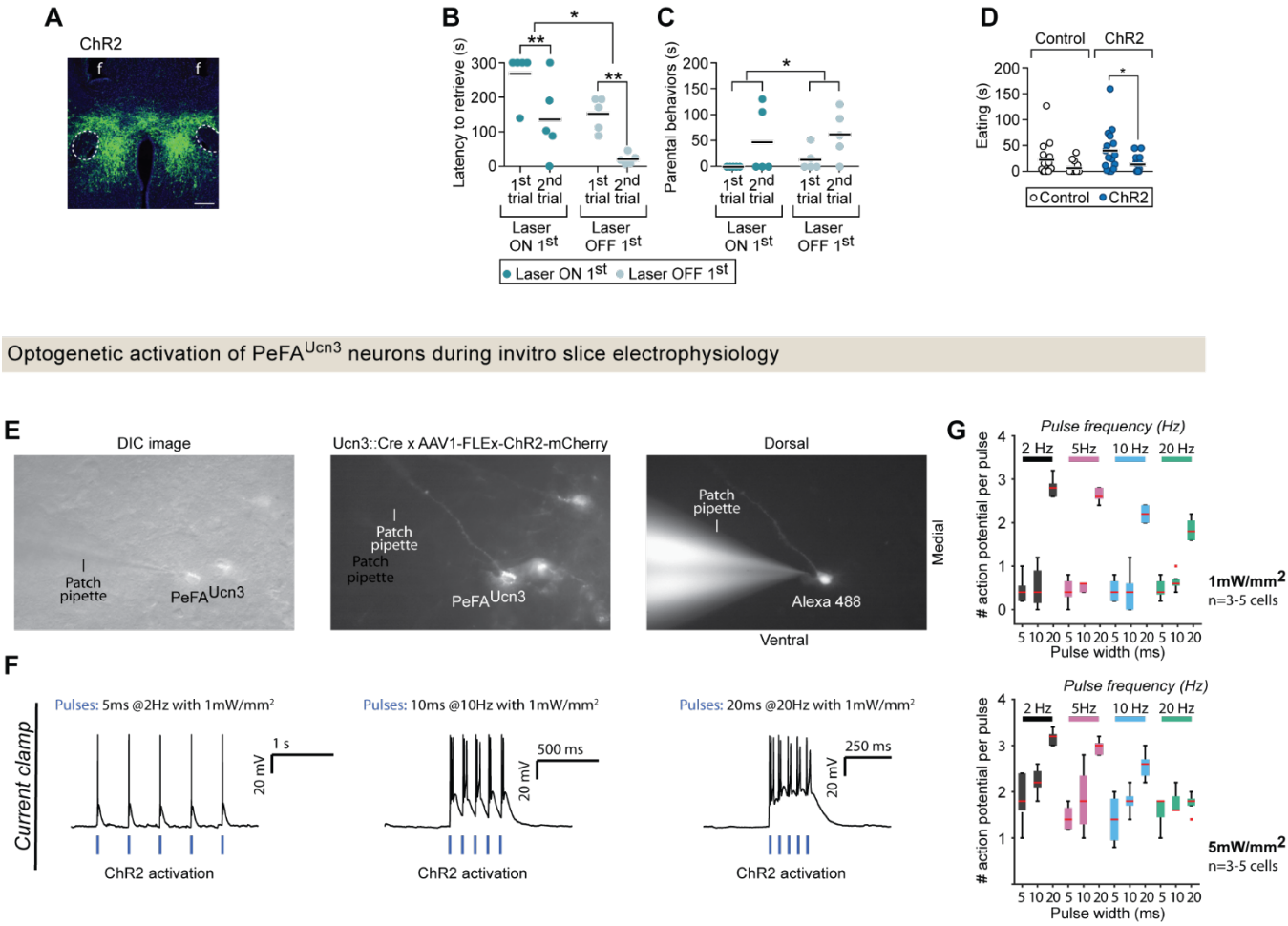

Figure 3—figure supplement 3.

A. Representative image of viral mediated ChR2 expression in the PeFA of Ucn3::Cre virgin females (scale bar 100 μm). Fornix indicated by outline, arrowhead indicates ventricle, f denotes fiber tract. B. Latency to retrieve pups in virgin females injected with ChR2 in either laser ON first conditions (dark green dots; n=5) or laser OFF first conditions (light green dots; n=5). Two-way repeated measures ANOVA reveals a significant main effect of laser order $F_{1,8}$=8.235 p<0.02 and session $F_{(1,8)}$=39.16 p<0.0002, Sidak's multiple comparisons test for on first condition and off first condition significant. C. Parental behavior duration also showed a significant main effect of session $F_{1,8}$=6.519, p<0.034 with no significant post-hoc effects. D. Eating duration of an appetitive food was significantly altered with laser

treatment (two-way repeated measures ANOVA $F_{1,29}$=8.504, p<0.0068, Bonferroni's multiple comparisons ON vs. OFF for ChR2 group). E. Raw images depicting (left) DIC, (middle) PeFA^{Ucn3} neurons labelled with mCherry (Ucn3::Cre injected with AAV1-eF1a-DoubleFlox hChR2(H134R)-mCherry-WPRE-HgHpA, 8-12 weeks old male mice, n=2) and (right) a recorded PeFA^{Ucn3} neuron filled with Alexa 488 hydrazide. F. Single traces showing activation of ChR2 positive PeFA^{Ucn3} neurons for (left) 5 ms light pulses at 2Hz and 1 mW/mm2, (middle) 10 ms light pulses at 10Hz and 1 mW/mm2, (left) 20 ms light pulses at 20Hz and 1 mW/mm2 from a custom-built 465 nm (1-5mW/mm2, CBT-90-B-L11, Luminus) light source. G. Summary data showing the activation of ChR2 positive PeFA^{Ucn3} neurons (n=5 neurons) in response to different pulse widths (5, 10, 20 ms) for four different stimulation frequencies; 2 Hz (black), 5 Hz (pink), 10 Hz (blue) and 20 Hz (green) for 2 different stimulation intensities of 1 mW/mm2 (top) and 5 mW/mm2 (bottom).

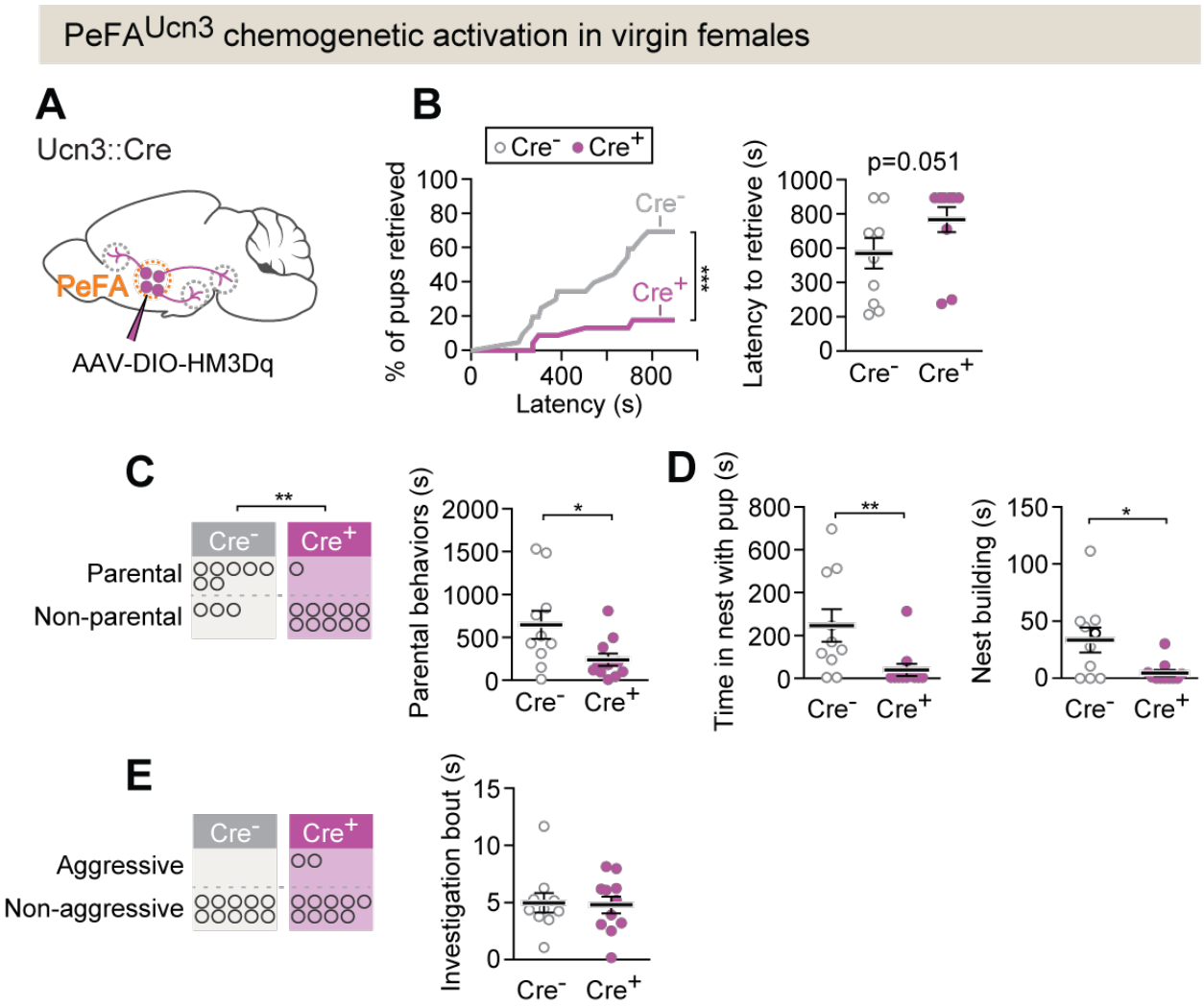

Figure 4. PeFA^{Ucn3} chemogenetic activation in virgin females suppresses parental behavior.

A. Setup for chemogenetic activation of PeFA^{Ucn3} neurons in virgin females. B. (left) Cumulative retrieval in Cre+ (n=11) or Cre- control (n=10) females. Kolmogorov-Smirnov test for significance p<0.0001. (right) Latency to retrieve first pup, Mann-Whitney test p=0.051. C. (Left) Number of females in Cre+ or Cre- (control) displaying parental behaviors. Significance determined by Fisher's exact test (p=0.0075). (right) Duration of parental behaviors, t-test p<0.0291. D. (left) Duration in nest, Mann-Whitney test, p=0.0039. (right) Nest building, Mann-Whitney test p=0.0422. E. (left) Number of females in Cre+ or Cre - (control) displaying infant-directed aggression. (right). Investigation bout length is unaffected.

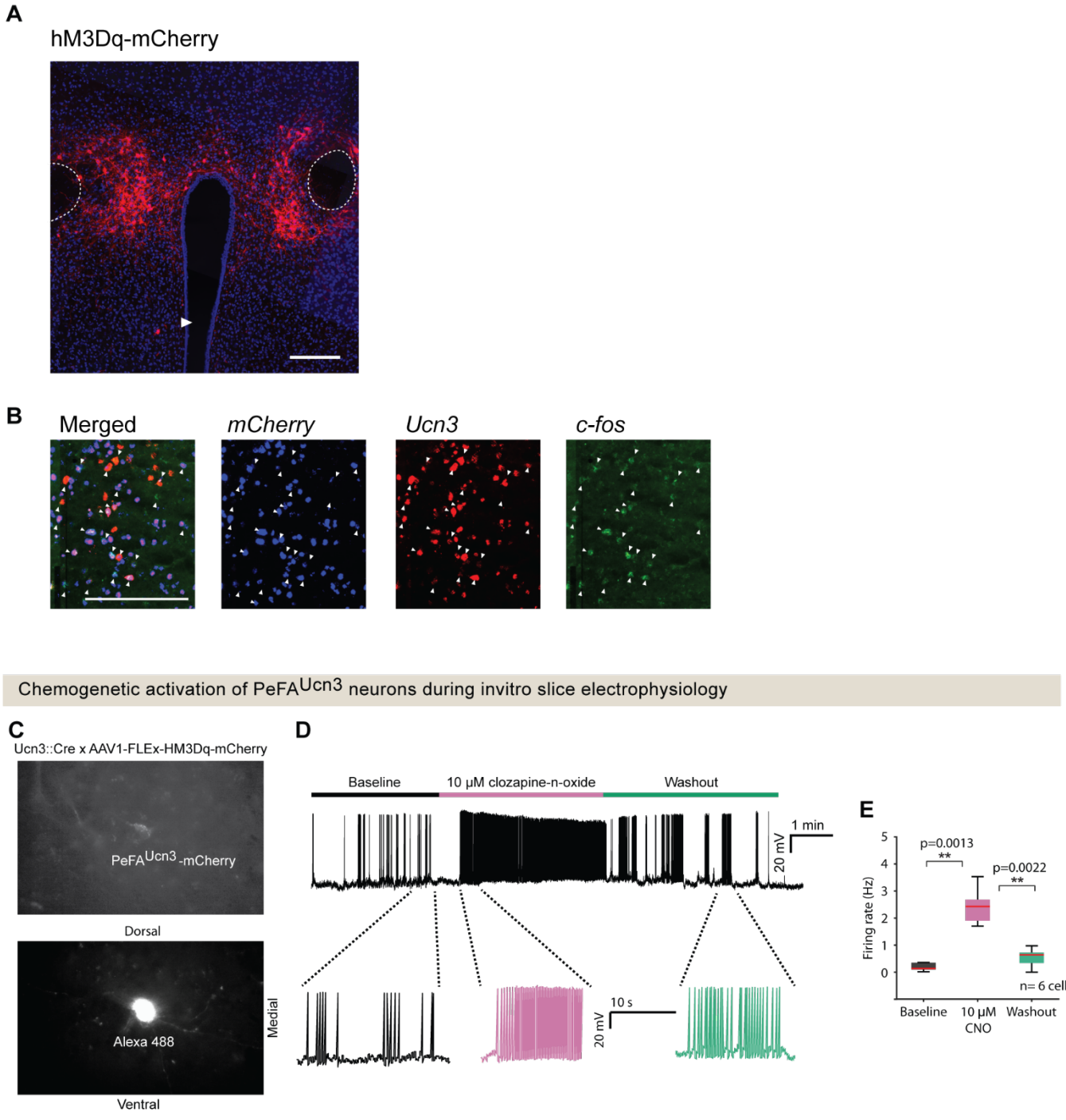

Figure 4—figure supplement 4.

A. Representative fluorescence image of excitatory DREADD (hM3Dq) viral-mediated expression in the PeFA of a Ucn3::Cre virgin female (scale bar 100 μm) Fornix indicated by outline, arrowhead indicates

ventricle. B. Representative *in situ* hybridization images of *mCherry*, *Ucn3*, and *c-fos* in a Ucn3::Cre virgin female 30 minutes after treatment with 0.3 mg/kg CNO (scale bar 100 μm), arrowheads indicate colocalization. C. Fluorescence images showing (top) $PeFA^{Ucn3}$ neurons labelled with mCherry (Ucn3::Cre male mice injected with pAAV-hSyn-DIO-hM3D(Gq)-mCherry) and (bottom) a recorded $PeFA^{Ucn3}$ neuron filled with Alexa 488 hydrazide. D. Example trace of a $PeFA^{Ucn3}$ neuron with bath application of CNO (3-5 minutes of baseline followed by 3-5 minutes of bath application of 10 μM CNO and 3-5 minutes of washout of CNO). E, Summary plot showing significant increase in the firing rate of the neurons ($p= 0.0013$ and 0.0022 compared to baseline and washout, Wilcoxon rank sum method) in response to application of CNO (6 cells for 8-12 weeks old male mice, n=2 animals).

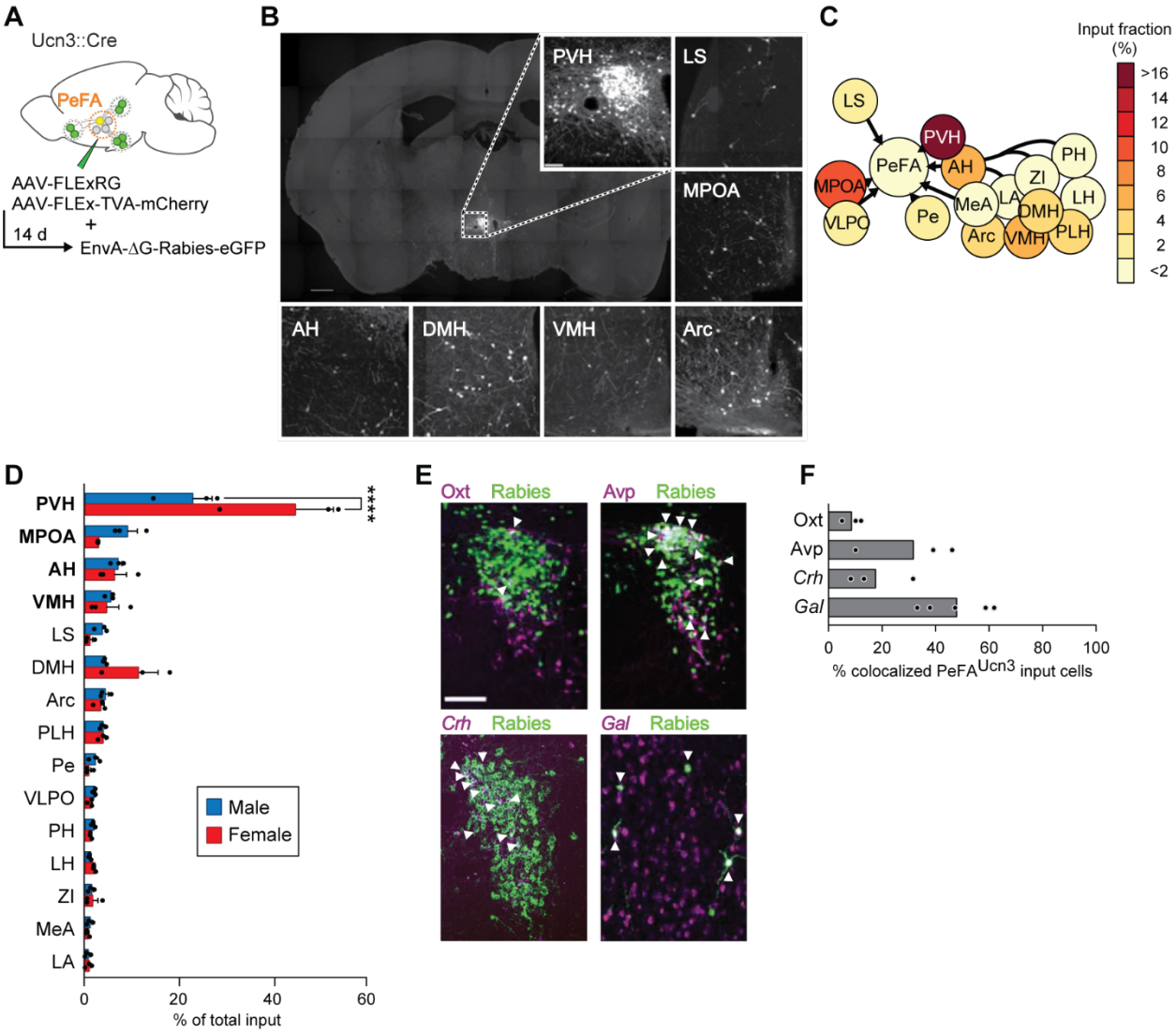

Figure 5. Inputs of PeFA^{Ucn3} neurons.

A. Schematic of monosynaptic retrograde tracing from PeFA^{Ucn3} neurons. B. Representative images of labeled monosynaptic inputs (scale bar 200 μm). C. Heatmap of input fractions by brain area in virgin males. D. Quantification of input fraction in virgin males (n=3) and virgin females (n=3). Regions are ranked by effect size largest (top) to smallest (bottom) relative to values observed in males using a regression analysis. PVH and MPOA, and to a lesser extent AH and VMH, showed significantly enriched input to the PeFA^{Ucn3} neurons compared to chance ($p<0.0001$, indicated in bold), *post-hoc* test significant for PVH male vs. female. E. Representative images of immunofluorescence (Oxt, Avp) or in situ

hybridization (corticotropin-releasing hormone *Crh*, *Gal*) co-staining with Rabies-eGFP (scale bar, 200 μm), arrowheads indicate colocalization. F. Percentages of presynaptic eGFP positive neurons expressing Oxt, Avp, *Crh* or *Gal* (n=3-5/group). MPOA input neurons largely colocalize with galanin expression (48.02 ± 5.63%).

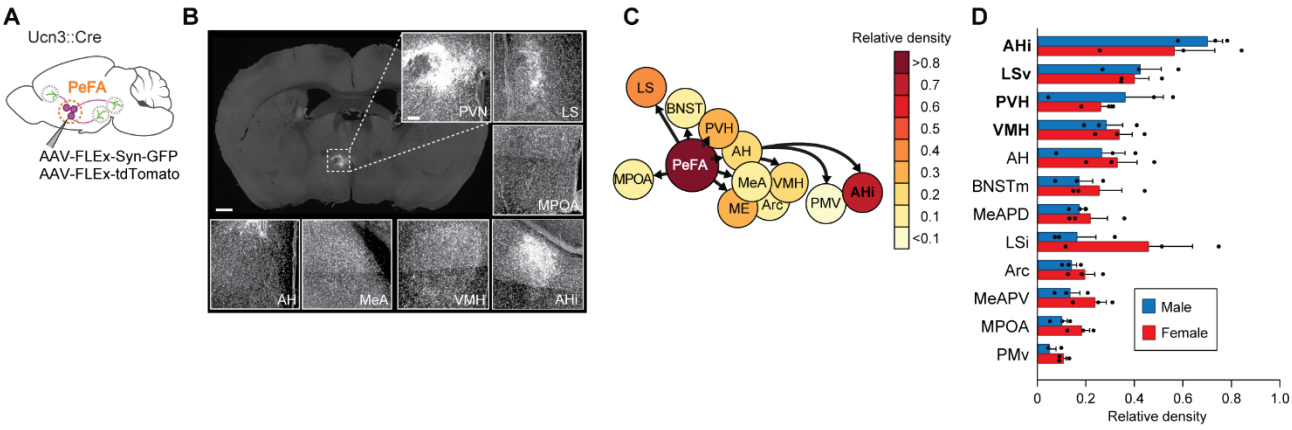

Figure 6. Projections of PeFA^{Ucn3} neurons.

A. Anterograde tracing strategy. B. Representative images of synaptophysin densities in projection areas (scale bar 200 μm). C. Heatmap of relative densities of PeFA^{Ucn3} projections. D. Quantification of relative densities of PeFA^{Ucn3} projections in males (n=3) and females (n=3), regression analysis reveals significant enrichment of AHi, LSv, PVH, and VMH projections compared to chance (indicated in bold).

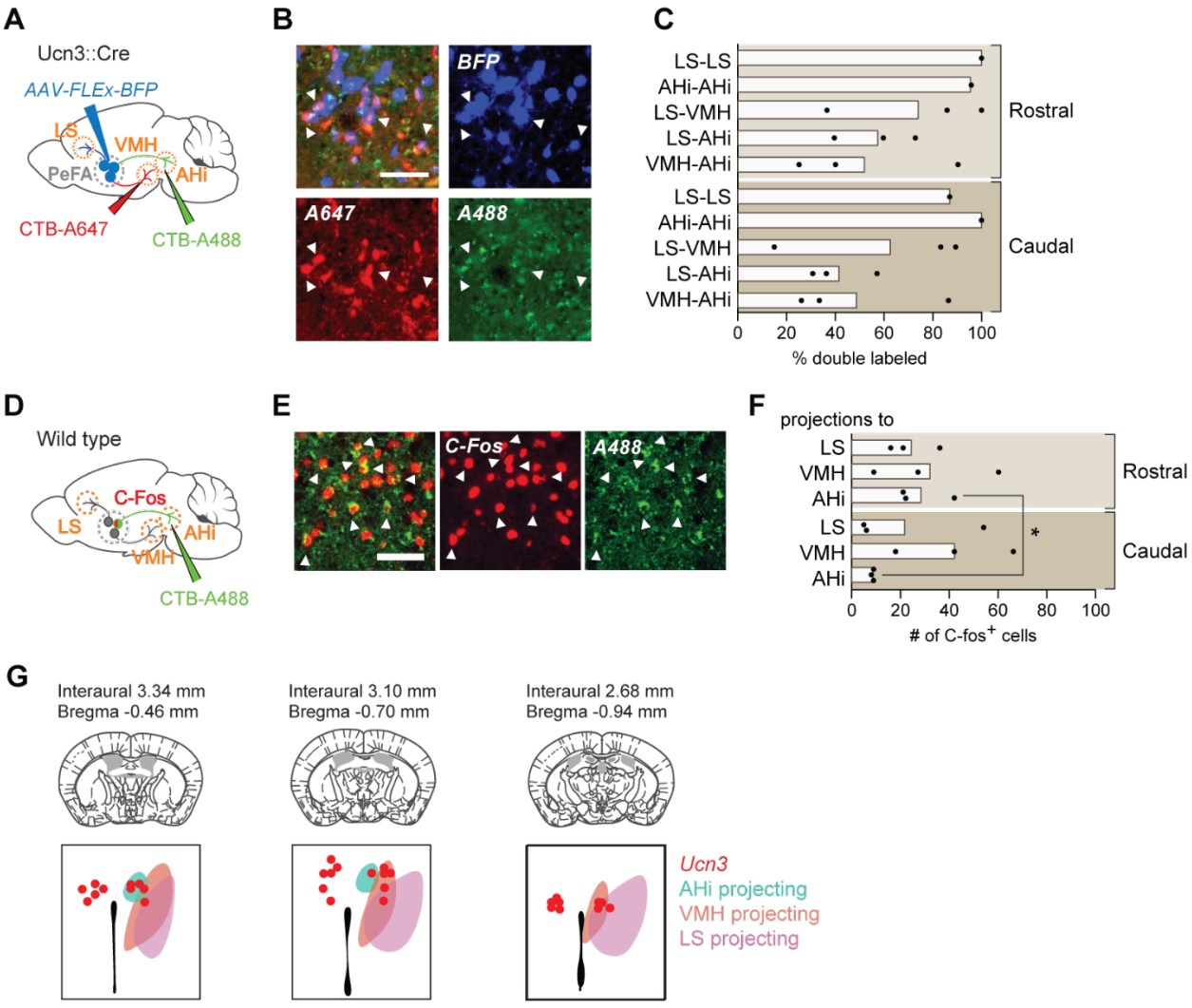

Figure 7. Projection tracing reveals bifurcating but behaviorally-distinguishable sub-populations of PeFA^{Ucn3} neurons. A. Schematic of retrograde CTB tracing combined with PeFA^{Ucn3} reporter. B. Representative image of CTB experiment (scale bar 100 μm). C. Quantification of *Ucn3*+ neurons labeled with CTB. D. Schematic of CTB tracing combined with C-Fos staining in infanticidal males. E. Representative image of CTB and C-Fos labeling in PeFA after CTB injection in AHi. F. Quantification of number of C-Fos positive cells labeled with CTB in the rostral and caudal PeFA after CTB injection in a given projection (n=3/group). Rostral versus caudal percentages are significantly different for AHi-

projecting neurons (paired t-test $p<0.03$). G. Schematic of topographical arrangement of $PeFA^{ucn3}$ neurons in PeFA according to their projection sites.

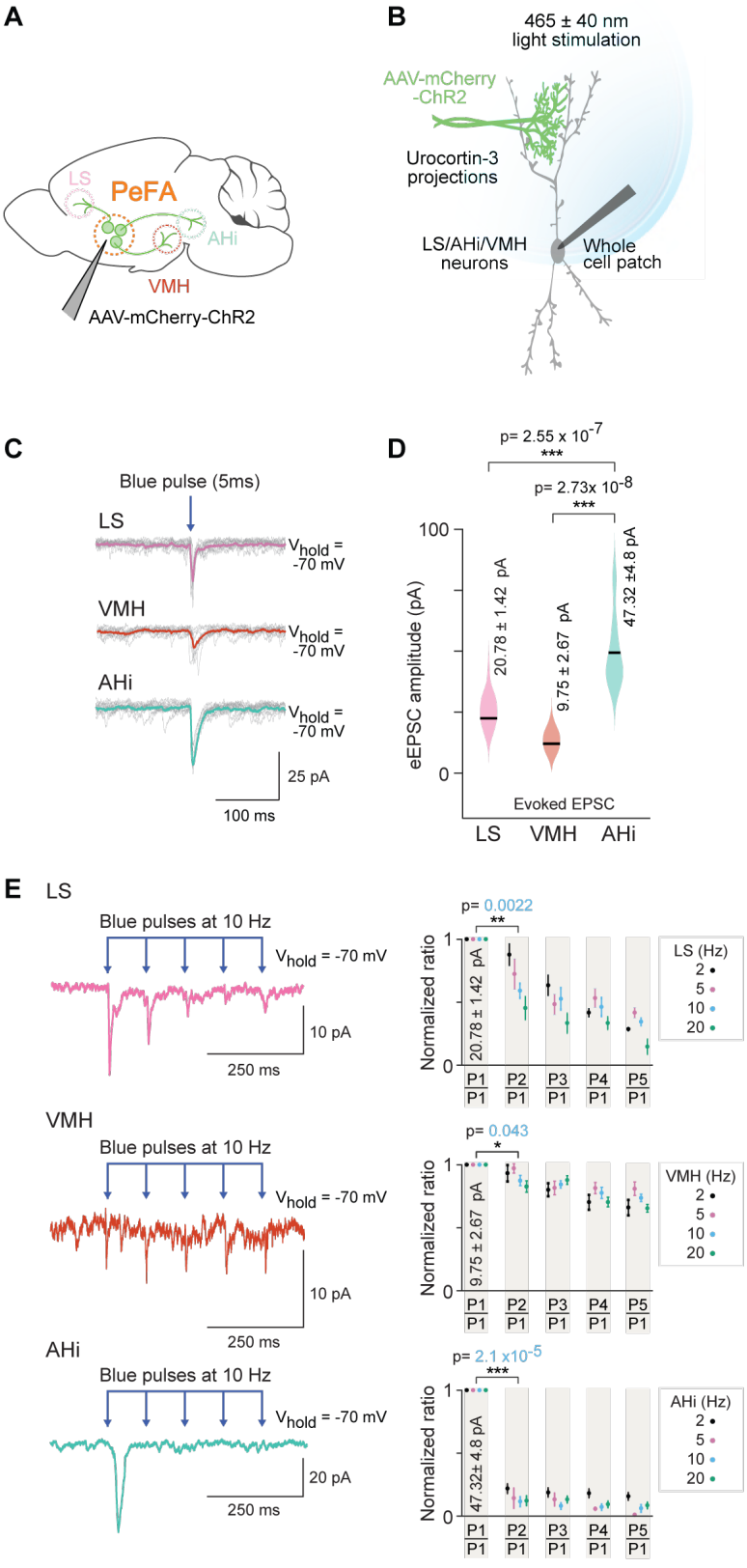

Figure 8. Optogenetic investigation of functional connectivity between PeFA^{Ucn3} neurons and specific targets.

A. Experimental design depicting selective targeting of PeFA^{Ucn3} with ChR2 (Ucn3::Cre injected with AAV1-eF1a-DoubleFlox hChR2(H134R)-mCherry-WPRE-HgHpA, 8-12 weeks old male mice, n=8, 5 males and 3 females). B. Schematic depicting in vitro slice electrophysiological recordings of neurons in LS, VMH and AHi slices in response to optogenetic activation of PeFA^{Ucn3} projections labelled with ChR2. C. Electrophysiological responses to activation of PeFA^{Ucn3} projections (single light pulse: 5 ms duration, 465 nm at 5mW/mm^2) for 10 trials with average traces shown in pink (LS), orange (VMH) and green (Ahi). D. Summary plot showing significantly higher amplitude of evoked excitatory post-synaptic currents (eEPSCs) in neuronal populations of AHi (green) compared to LS (pink) (Wilcoxon rank sum test, $p<0.0001$) and VMH (orange) (Wilcoxon rank sum test, $p<0.0001$). E. Electrophysiological trace of a LS neuron (top left), a VMH neuron (middle left) and an AHi neuron (bottom left) (mean response of 5 consecutive trials) depicting paired pulse depression of EPSCs in response to activation of PeFA^{Ucn3} projections (light pulses: 5 ms duration, 465 nm at 10 Hz).Summary plots showing paired pulse depression of optogenetic activation of PeFA^{Ucn3} projections on LS neurons (top right, Wilcoxon rank sum test, $p=0.0022$), VMH neurons (middle right, Wilcoxon rank sum test, $p=0.043$) and AHi neurons (bottom right, Wilcoxon rank sum test, $p<0.001$) as a function of stimulation frequency.

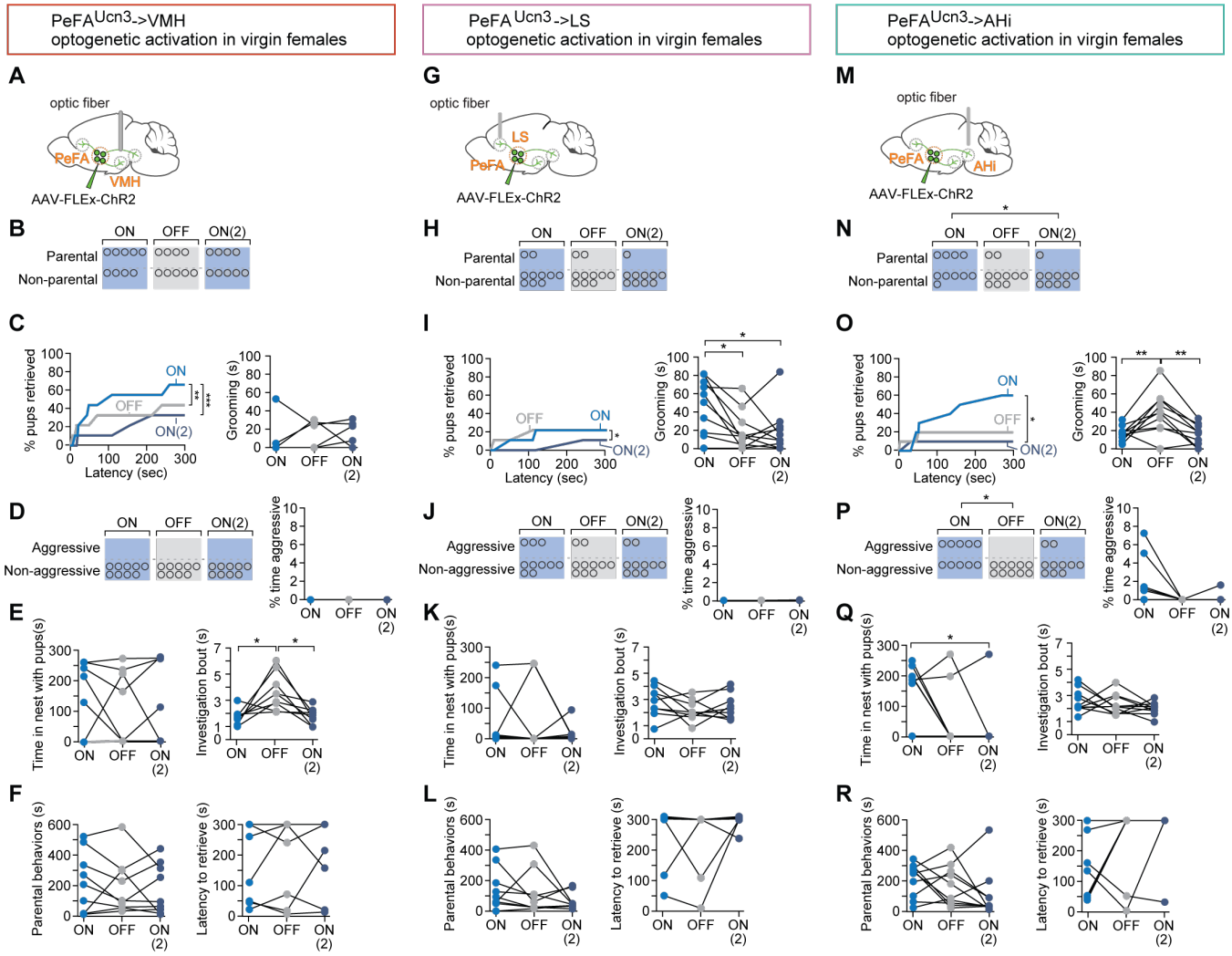

Figure 9. Specific projections from PeFA^{Ucn3} neurons mediate infant-directed neglect and aggression.

A. Optogenetic stimulation of PeFA^{Ucn3} to VMH fiber terminals. B. Number of females showing parental behavior. C. (left) Cumulative retrieval of pups is significantly different among groups (Friedman statistic $_{(3-15)}$ = 19.57, p<0.0001; n=9). Dunn's multiple comparisons test reveals difference between ON vs. ON2 (***) and OFF vs. ON2 (*). (right) One-way repeated measures ANOVA revealed a significant main effect in investigation bout length $F_{(1, 11)}$=10.12 (p<0.005) among groups. Tukey's multiple comparisons revealed differences between ON vs. OFF (*) and OFF vs. ON2 (*). D. (left) Number of females showing pup-directed aggression and (right) percent time displaying aggression show no differences across sessions. E. (left) Time in the nest with pups and (right) grooming were not altered by PeFA^{Ucn3} to VMH fiber stimulation. F. (left) Duration of parental behaviors and (right) latency to retrieve pups were not changed. G. Optogenetic stimulation of PeFA^{Ucn3} to LS terminals. H. Number of females showing parental behavior is not affected (n=10). I. (left) Cumulative retrieval of pups is suppressed and significantly affected over the course of the experiment analyzed by Friedman test, Friedman statistic $_{(3-7)}$= 10.21 (p<0.0041). Dunn's multiple comparisons test reveals significant differences in OFF vs. ON2 comparison (*). (right) One-way repeated measures ANOVA reveals that grooming is significantly reduced over the course of the experiment F_{2-16}=6.368 (p<0.0102). Tukey's multiple comparisons test reveals significant differences between ON vs. OFF (*) and ON vs. ON2 (*). J. (left) Number of females showing aggression and (left) time spent aggressive toward pups is not changed. K. (left) Time in the nest and (right) investigation bout length are not affected. L. (left) Parental behaviors and (right) latency to retrieve are unaffected. M. Schematic of optogenetic stimulation of PeFA^{Ucn3} to AHi terminal stimulation. N. Number of females showing parental behaviors was significant reduced between ON v. ON2 conditions (Chi-square p<0.0191). (right) One-way repeated measures ANOVA revealed reversibly reduced grooming by stimulating of PeFA^{Ucn3} to AHi axonal terminals $F_{2,18}$=11.40 (p<0.0006). Tukey's multiple comparisons test showed differences between ON vs. OFF (**) and OFF vs. ON2 (**). O. (left) Friedman test reveals that cumulative retrieval of pups is significantly affected (p<0.0095). Dunn's multiple comparisons shows significant differences between ON vs. ON2 (*). (right) Time spent in the nest with pups was significantly reduced between ON vs. ON2 conditions (Repeated measures ANOVA $F_{2,14}$=4.297 p<0.0351, followed by Tukey's

post-hoc test). P. (left) Number of females showing aggressive behaviors toward pups is significantly different between laser on and laser off groups (Chi-square test $p<0.02$; $n=10$). (right) Friedman test reveals a significant difference in the time spent displaying aggressive behavior over the course of the experiment ($p<0.0247$). Q. (left) Time spent in the nest with pups was significantly reduced between ON vs. ON2 conditions (Repeated measures ANOVA $F_{(2,14)}=4.297$ $p<0.0351$, followed by Tukey's post-hoc test) (right) and investigation bout length were unaffected. R. (Left) Duration of parental behaviors and (right) latency to retrieve were unchanged across sessions.

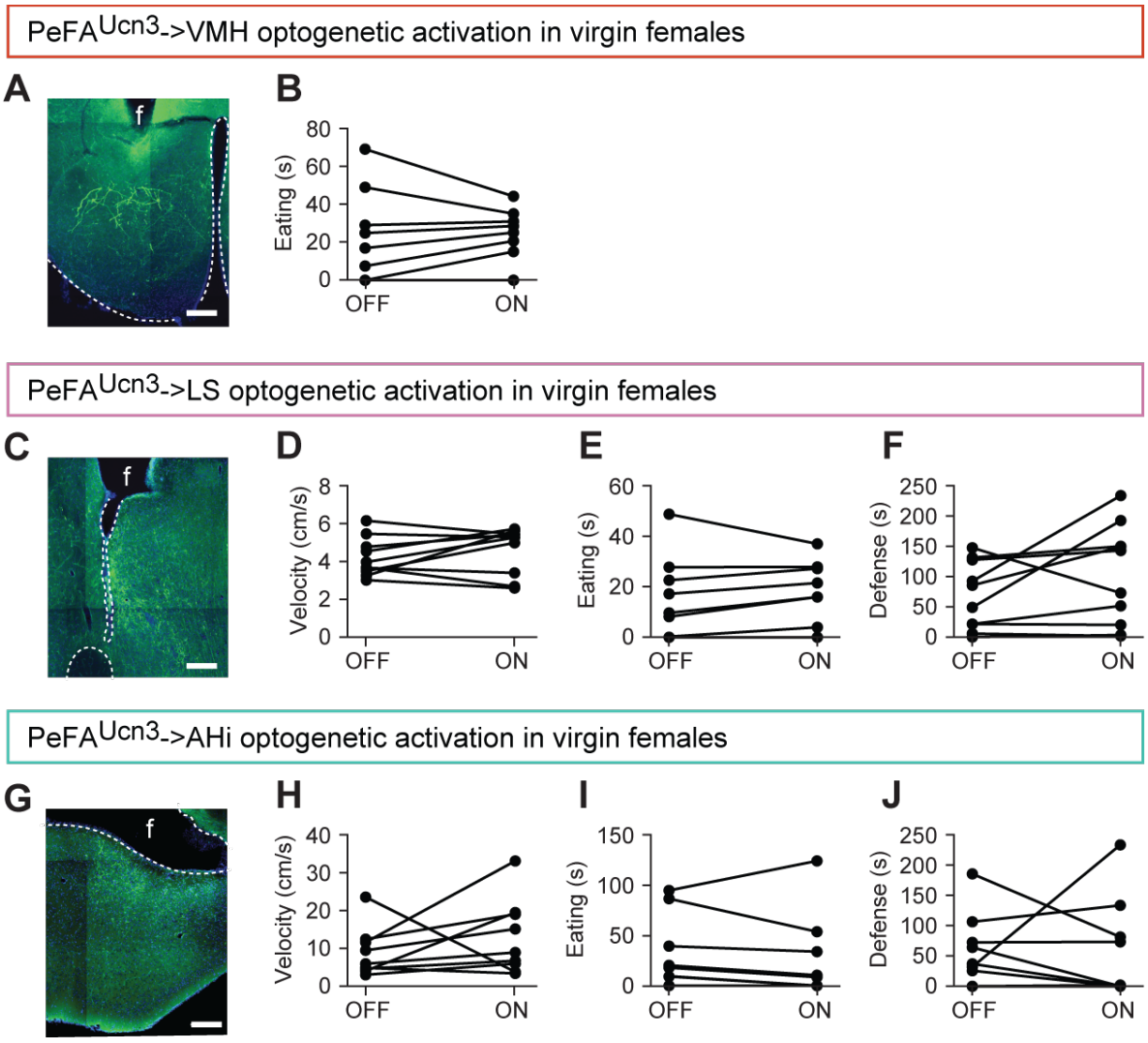

Figure 9—figure supplement 9.

A. Representative image of viral mediated ChR2 expression in Ucn3::Cre virgin females with fiber implant (f) directed toward the VMH, scale bar 100 μm, ventricle outlined. B. Time spent eating a cookie was not affected by laser condition (n=8). C. Representative image of viral mediated ChR2 expression in Ucn3::Cre virgin females with fiber implant (f) directed toward the LS scale bar 100 μm, ventricle outlined. D. Velocity in locomotion test (n=10). E. Time spent eating a cookie (n=9). F. Time spent showing defensive behavior toward a castrated male intruder swabbed with intact male urine (n=10). G. Representative image of viral mediated ChR2 expression in Ucn3::Cre virgin females with fiber implant (f) directed toward the AHi, scale bar 100μm, ventricle outlined. H. Velocity in locomotion test (n=9). I.

Time spent eating a cookie (n=9). J. Time spent showing defensive behavior toward a castrated male intruder swabbed with intact male urine (n=9).

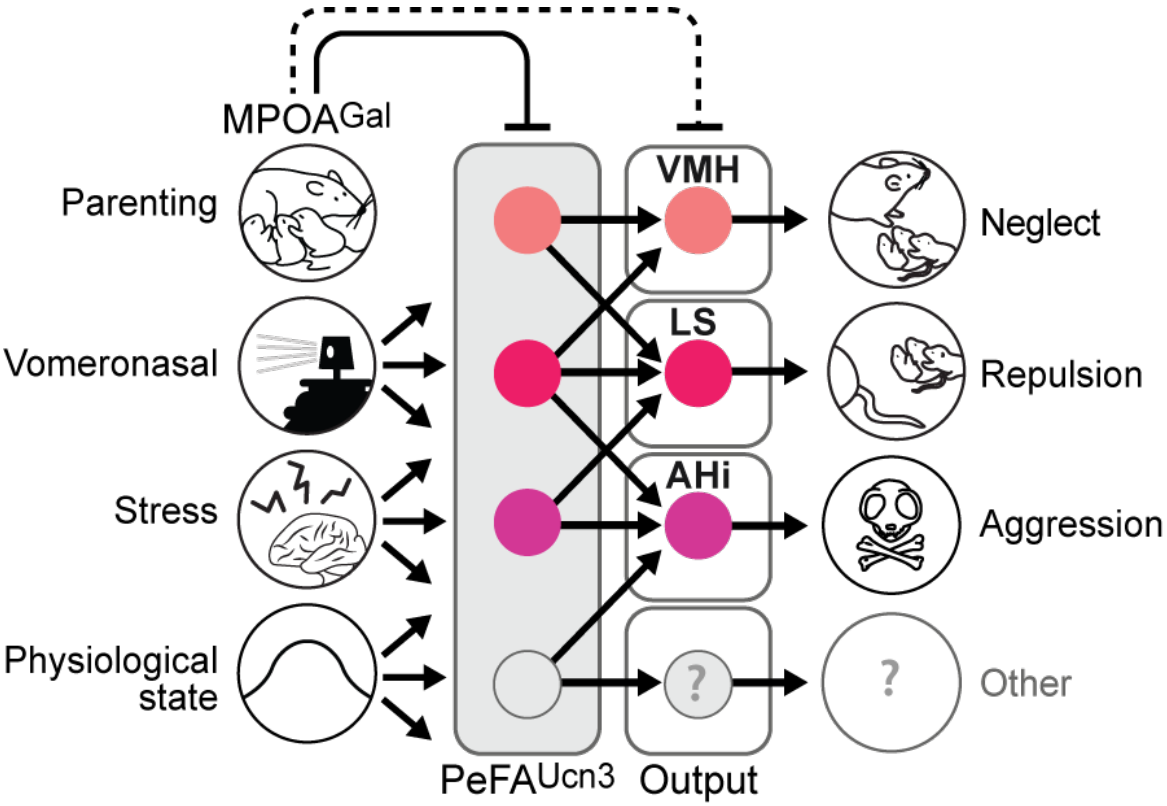

Figure 10. Model of the organization and function of PeFA^{Ucn3} neurons in infant-mediated neglect and aggression

PeFA^{Ucn3} neurons receive input from brain areas involved in processing social cues and physiological state, stress as well as parenting control. In turn, PeFA^{Ucn3} neurons send bifurcating projections to major targets such as the AHi, LS, and VMH. Stimulation of these projections specifically impact various aspects and degrees of pup-directed agonistic behavior from avoidance (VMH), repulsion (LS), to aggression (AHi).

Supplementary Videos:

Supplementary video 1: Optogenetic stimulation of PeFA^{Ucn3} neurons in a virgin female mouse during pup-directed behavior. A newborn pup is presented to a female in the home cage. Optogenetic stimulation is indicated by the white dot in the upper center of the frame. In a subset of females, we observe tail rattling behavior toward the pup during light illumination as seen in this example.

Supplementary video 2: Optogenetic stimulation of PeFA^{Ucn3} neuronal projections to the ventromedial hypothalamus in a virgin female mouse during pup-directed behavior. Most females showed reduced interaction with the pup during light illumination as seen here.

Supplementary video 3: Optogenetic stimulation of PeFA^{Ucn3} neuronal projections to the lateral septum in a virgin female mouse during pup-directed behavior. Most females showed avoidance of the pup during light illumination, and in a subset of females we observed escape-like behavior upon light stimulation as in this example.

Supplementary video 4: Optogenetic stimulation of PeFA^{Ucn3} neuronal projections to the amygdalohippocampal area in a virgin female mouse during pup-directed behavior. Most females showed reduced parental behavior toward pups, and a subset of females displayed pup-directed aggression such as aggressively carrying the pups around the cage without retrieving upon light illumination as in this example.